TR 24

UT-IG - Tech. Report #24

Technical Report
Daule - Peripa Seismograph Network
June 1, 1983

Submitted to:

Ing. Marco Dominguez Plaza
Director Proyecto Daule - Peripa
CEDEGE
Guayaquil, Ecuador

and

Tippets - Abbett - McCarthy - Stratton
Engineers & Architects
The Tams Building
655 Third Avenue
New York, N.Y. 10017

Prepared by:

Dr. Tosimatu Matumoto
Institute for Geophysics
University of Texas at Austin
4920 North IH 35
Austin, Texas 78751

Dr. Wayne Pennington
Department of Geological Sciences
University of Texas at Austin
Austin, Texas 78712

Institute for Geophysics
Contribution No. 558

CONTENTS

Introduction

At the conclusion of the first 2 years of the seismic monitoring program, this technical report was prepared:

(1) To review the seismic studies in northeastern South America.

(2) To review the installation and subsequent performance of the network.

(3) To extract some of the conclusions on the seismicity based on the recorded events by the Daule - Peripa Seismograph Network.

1. GEOLOGY AND TECTONIC SETTING

1.1. Geology in Ecuador

The Republic of Ecuador straddles the equator on the Pacific coast of South America and is made up of three physiographic provinces; the coastal lowlands, the Andean mountain chains and the Orient province in the Amazon headwaters. Geologically, the country extends from the oceanic province of the Pacific, across the Andean mobile belt to the margins of the Precambrian Guayana Shield in the east. (see Figure 1A). It forms the southern part of the Northern Andes, a fold belt that swings northward through Colombia and Venezuela to connect with the Antillean arc.

Ecuador is divisable into two major geological provinces, i.e., Eastern and Western provinces. In the Eastern province, a basement of Precambrian igneous and metamorphic rocks belonging to the Guayana Shield is overlain by a relatively complete sequence of Phanerozoic sediments. In the Western province, on the other hand, the basement appears to be represented by a Mesozoic sequence of eugeosynclinal and oceanic rocks, capped by a comparatively thin Tertiary succession. The boundary between the two provinces is drawn along a postulated magashear, comprising the Guayaquil and Dolores faults, which may utlimately connect with Oca-Pilar faults to make up a major dextral shear zone bordering the South American continent.

Ecuador can be divided into 9 different structural zones: Western Littoral and Continental Shelf, Gulf of Guayaquil Province, Pacific Coast Range, Coastal Depression, Western Andes, Quito-Cuenca Depression, Cordillera Real, Eastern Andes and Oriente Basin and Guayana Shield

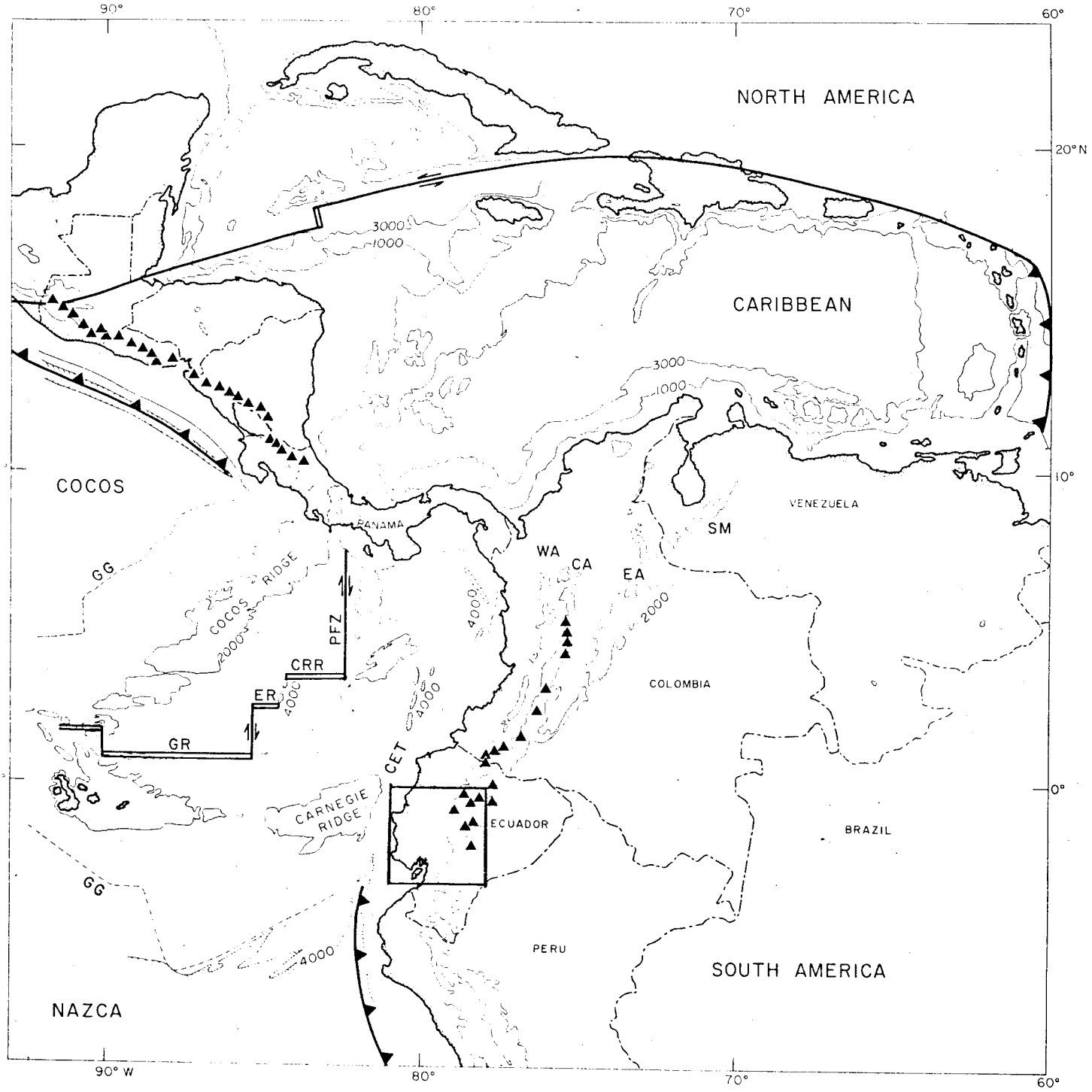

Fig. 1A. Major features of northwestern South America. The box outlines area of maps for station-locations seismicity determined from the local network. Triangles indicate volcanoes. GR: Galapagos rift CRR: Costa Rica rift PFZ: Panama Fracture Zone CET: Colombia-Ecuador Trench WA, CA, EA: Western, Central, and Eastern Andes.

(margin). Brief discussions on characteristics of these zones are given here. Guayana Shield is a stable block of Precambrian igneous and metamorphic rocks capped by a thin veneer of Panerozoic continental sediments. The Oriente Basin is a segment of the Subandean province that separates the Guayana Shield from the Andean mobile belt. The Cordillera Real forms the core of the Andes, built of high-grade metamorphic rocks, but by intrusions, and in places capped by Quaternary volcanoes. The Quito-Cuenca depression is an intermontane graben separating the Cordilla Real from the Western Andes. It is cut by numerous faults belonging to the Dolores-Guayaquil fault system. Faults along its margins have caused lines of weakness along which volcanic rocks have reached the surface. The Dolores-Guayaquil fault cuts through the Western Andes at the latitutude of Guayaquil and divides the mountain chain into two discrete elements, i.e., the Cordillera Occidental in the north and the Amotape-Chanchan belt in the south. The Coastal Depression is a shallow depression in front of the Andes. The structure of this region is dominated by faulting, with broad flat-lying or gently synclinal regions being separated from one another by highly deformed faulted uplifts. The faults are linear and although causing intense local deformation, do not in general give rise to much stratigraphic separation, possibly an indication that they have a dominant transcurrent component. This structural pattern has been designated "shear folding" and appears to be characteristic of the circum-Pacific region. The Gulf of Guayquil province is a unique development on the west coast of South America. The Gulf of Guayaquil is the only major indentation on the west coast of South America and appears to be due to the interaction of two major fault systems. The first system is represented by the Romanche fracture zone in the Mid-Atlantic, the Amazon Basin which

separates the Guayana Shield from the Brazilian Shield; and the Galapagos fracture zone in the Pacific. The second system is represented by the Dolores-Guayaquil fault system which runs offshore at the Gulf of Guayaquil, apparently causing a destral offset to the Peru Trench (see Fig. 1B). Galapagos Islands, which are of volcanic origin, lie on the western end of a submarine uplift, the Carnegie Ridge and are bordered to the north by Galapagos fracture zone, a major E-W fault system. The islands are dominated by volcanic cones, crater lakes and lava fields.

1.2 Tectonic Setting

The western part of South America is one of the major plate boundaries where the oceanic Nazca plate in the west underthrusts the continent of South America. The outstanding feature of the continent is the high Andean belt, running close to its western border from eastern Venezuela to southern Chile (see Fig. 1B). This complex cordillera, often branching into several subparallel ranges, forms the division between the Pacific-Caribbean and Atlantic waterheads.

South of the equator along the Andean margin, the configuration of the Benioff zone is relatively well defined along the Peru and Chile trenches. Barazangi and Isacks (1976), by a detailed study of the spatial distribution of earthquakes that occurred between lat. 0° and 45°S, defined five segments of inclined seismic zones, in each of which the zones have relatively uniform dips. The segments beneath northern and central Peru (about lat. 2° to 15°S) and beneath central Chile (about lat 27° to 33°S) have very small dips (about 10°), whereas the three segments beneath Peru and northern Ecuador (about lat. 0° to 2°S), beneath southern Peru and northern Chile (about lat. 33° to 43°S) and

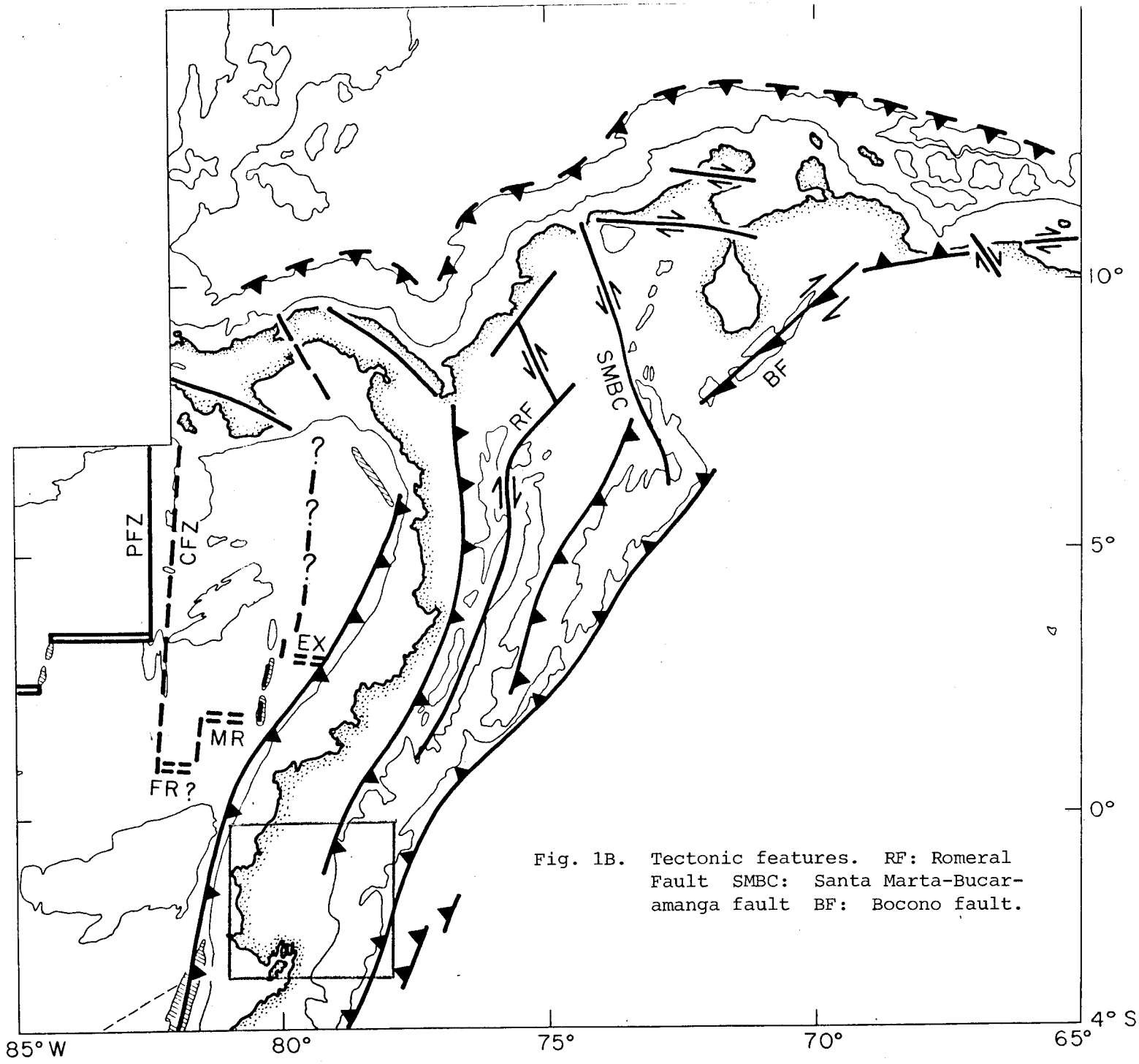

Fig. 1B. Tectonic features. RF: Romeral Fault SMBC: Santa Marta-Bucaramanga fault BF: Bocono fault.

beneath southern Chile (about lat 33° to 43°S) have steeper dips (25° to 30°). They found a gap in seismic activity between depths of 320 km and 525 km and a remarkable correlation between the two flat segments of the subducted Nazca plate and the absence of Quaternary volcanism on the South American plate. Fig. 1C shows that the study area is at a position of transition from a flat-lying now-volcanic zone to the south and a steeply dipping segment with volcanism to the north. Santo (1969) also found almost no seismic activity in the depth range from 320 km to 520 km for the seismicity in South America.

However, north of the equator along the Andean margin, subduction of oceanic lithosphere has been a matter of some controversy. Santo (1969) concluded that a south-dipping Benioff zone occurs beneath northern Colombia; Dewey (1972) suggested that a Benioff zone, if it exists, strikes N-S and dips to the east. Isacks and Molnar (1971) concluded that a Benioff zone exists, dipping to the east beneath Ecuador and the southeast beneath northern Colobmia. In a recent study, Pennington (1981) defined three segments in subducted lithosphere in this region; Bucaramanga, Cauca, and Ecuador segments (see Fig. 1D and 1E). The Bucaramanga segment (5.2°N to 11°N), dipping at 20° - 25° toward N109°E, contains the Bucaramanga nest of intermediate-depth earthquakes and is continuous with the Caribbean sea floor northwest of Colombia. The Cauca segment is separated from the Bucaramanga segment, to the south of 5.2°N, by a tear in the plate and dips at 35° toward N120°E. The subducted Cauca segment is continuous with the Nazca plate currently underthrusting South America at the Colombia-Ecuador trench. The Ecuador segment, beneath central and southern Ecuador, dips at 35° toward N35°E and is separated from the Cauca segment by a zone of very sparse intermediate-depth seismicity (see Fig. 1F).

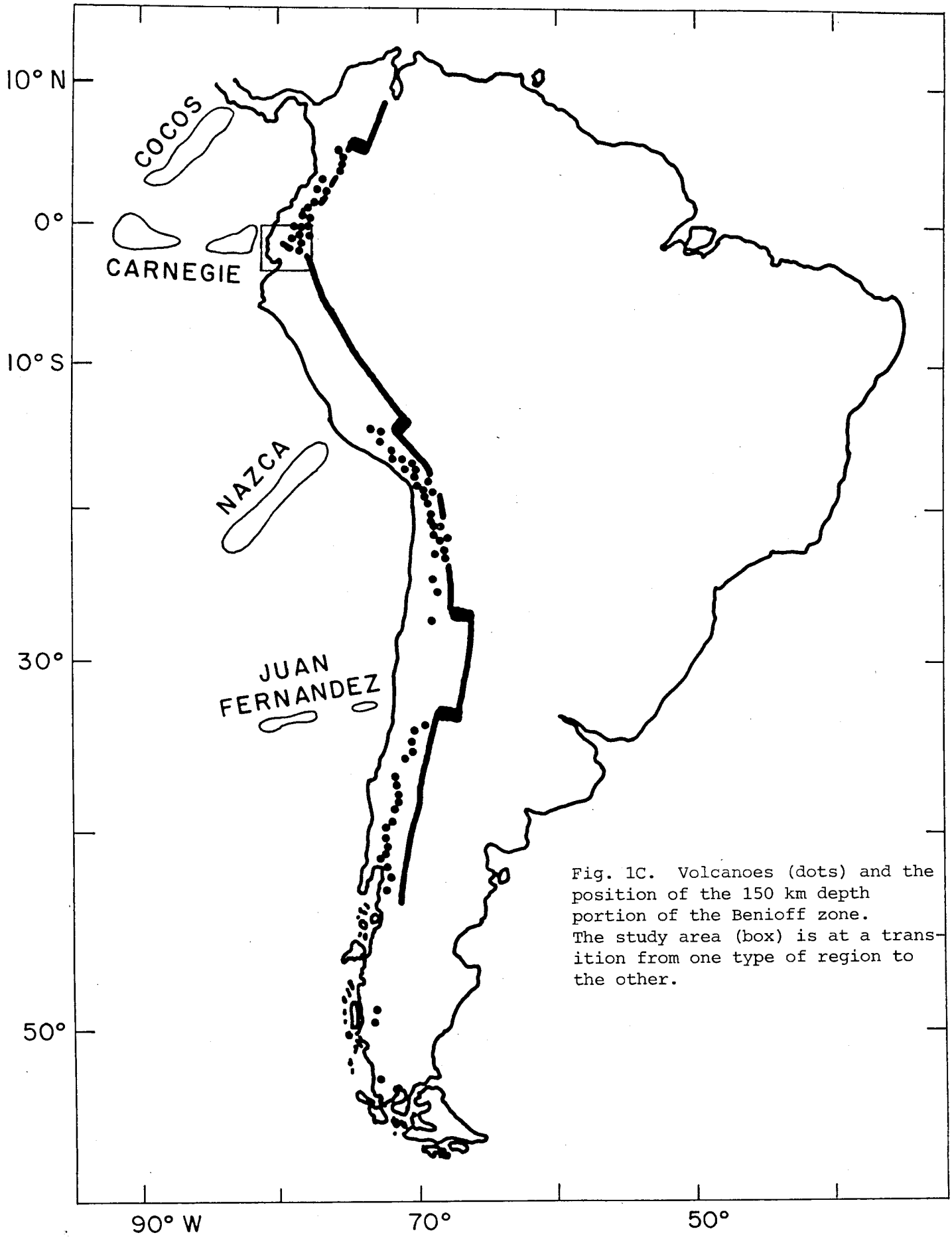

Fig. 1C. Volcanoes (dots) and the position of the 150 km depth portion of the Benioff zone. The study area (box) is at a transition from one type of region to the other.

Fig. 1D.
Intermediate-depth earthquake (from teleseismic observations) of northwestern South America. Three distinct segments are identified.

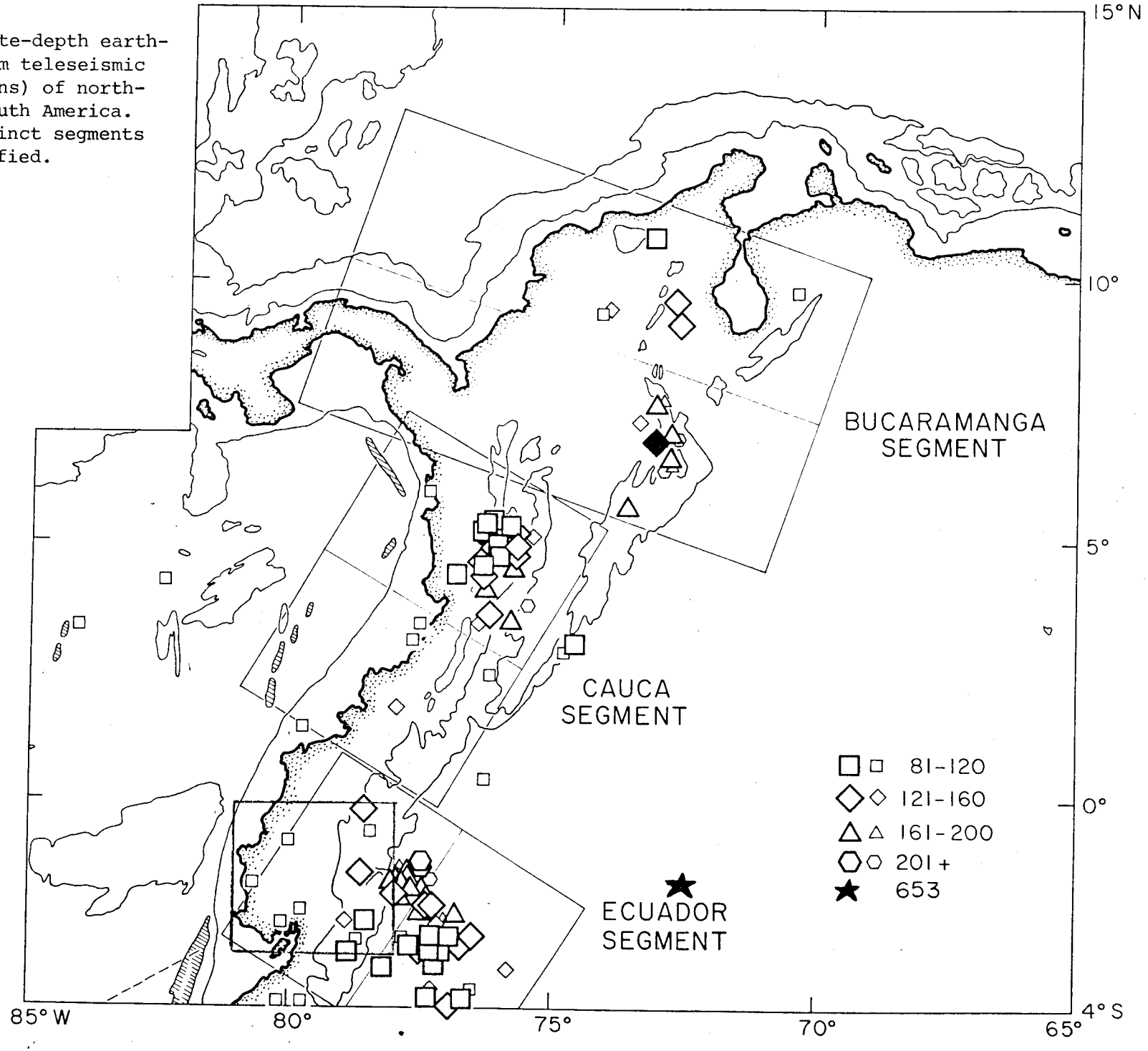

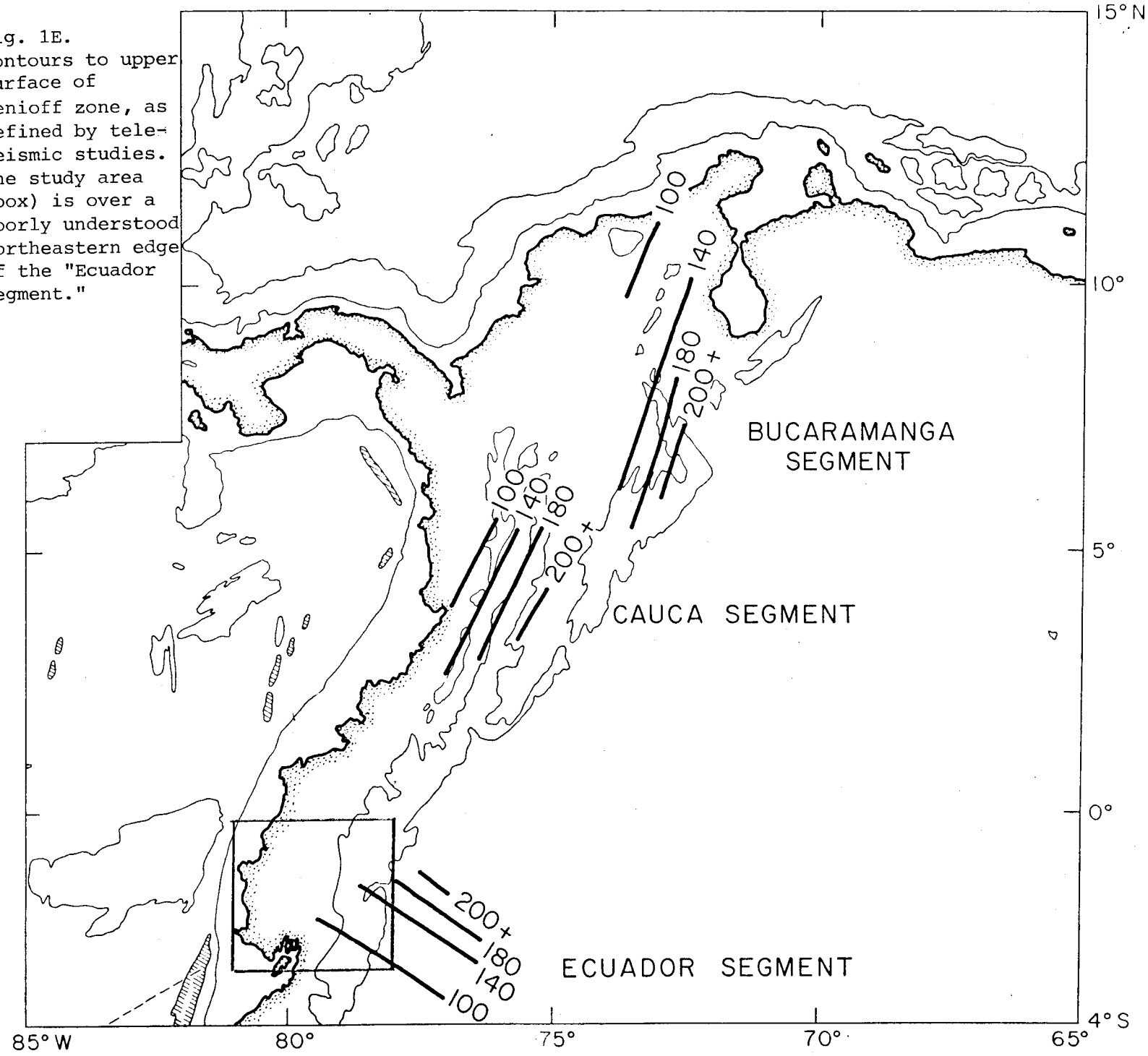

Fig. 1E.
Contours to upper surface of Benioff zone, as defined by teleseismic studies. The study area (box) is over a poorly understood northeastern edge of the "Ecuador segment."

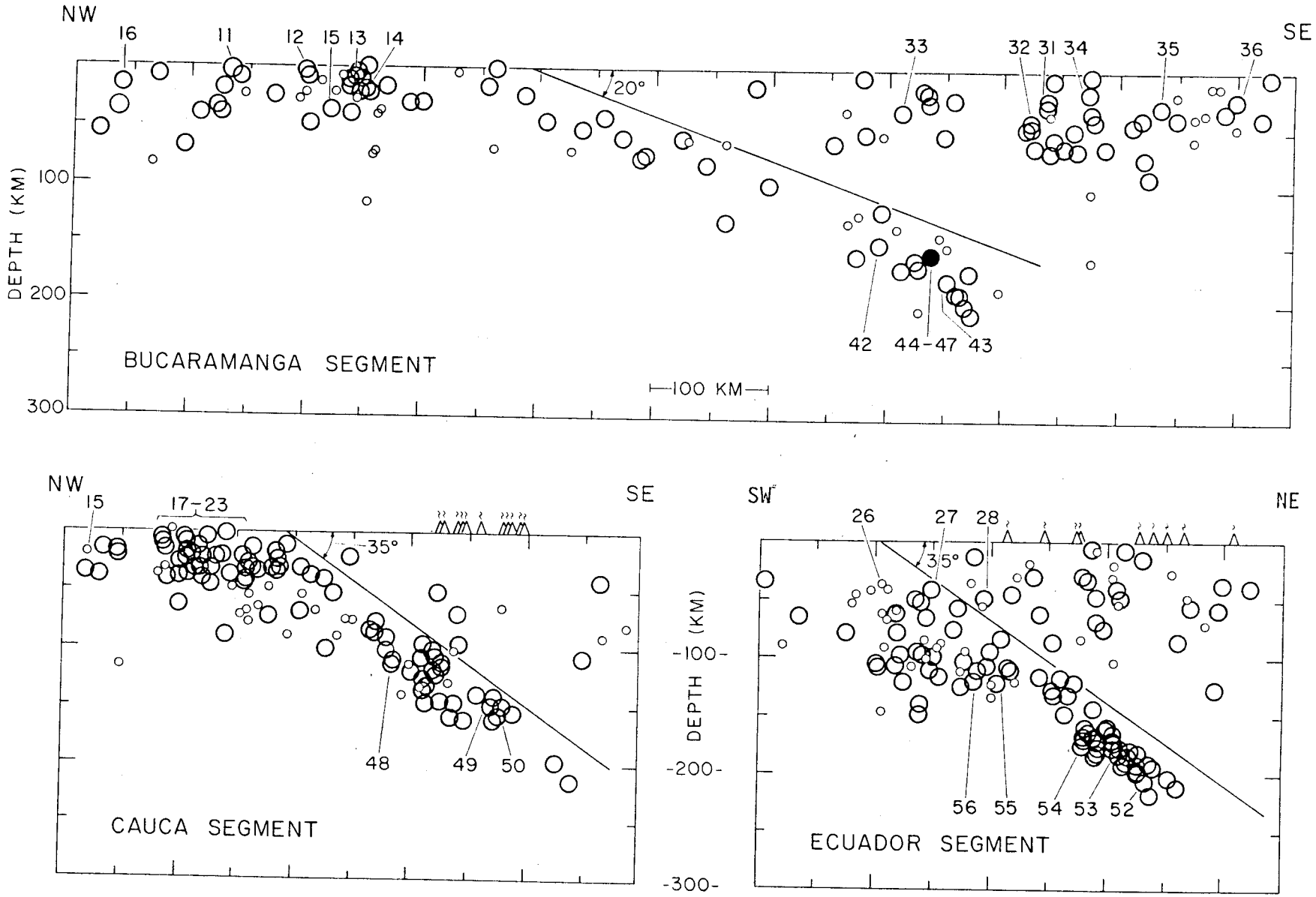

Fig. 1F. Cross-sections of seismicity from teleseismic observations. The Bucaramanga nest is the solid black dot (representing several hundred events) on the top diagram. The Cuenca nest is the cluster of events at 150-200 km depth in the Ecuador segment.

The Ecuador segment appears to be the northern end of the subducted Nazca plate beneath northern Peru (see Fig. 1G). From shallow seismicity (Fig. 1H) and focal mechanisms (Fig 1I), he found that the Andean block, the area between the Colombia-Ecuador trench and the eastern from of the Andes, is separated from the rest of South America by Eastern Andean Frontal Fault Zone and is moving NNE with respect to the rest of South America (Fig. 1J).

In northwestern South America, the Cocos, Nazca, South American, and Caribbean plates interact one another and generate very complicated plate boundaries which are not yeat fully understood. However, it is generally accepted that the Nazca and Caribbean plates are presently moving eastward with respect to South America, both the Nazca and South America plates are slowly converging with the Caribbean and the Cocos and Nazca plates are moving apart along the Galapagos ridge, which extends from Ecuador past the Galapagos Islands to a triple-point junction with the East Pacific rise. The Carnegie ridge is a "hot-spot trace" formed by excessive volcanism near the spreading center. The Galapagos Islands are a large archipelago with at least five active volcanoes, of which one had a caldera collapse in 1968. The simultaneous growth of the East Pacific rise and the Galapagos ridge are driving the Cocos plate northeastward into the Middle America trench which is very active in terms of seismic activity and volcanism.

2. SEISMICITY VIEWED FROM WWSSN DATA

2.1 General Seismicity in South America

The continental margin of the west coast of South America is one of the most seismically and tectonically active plate boundaries, with the

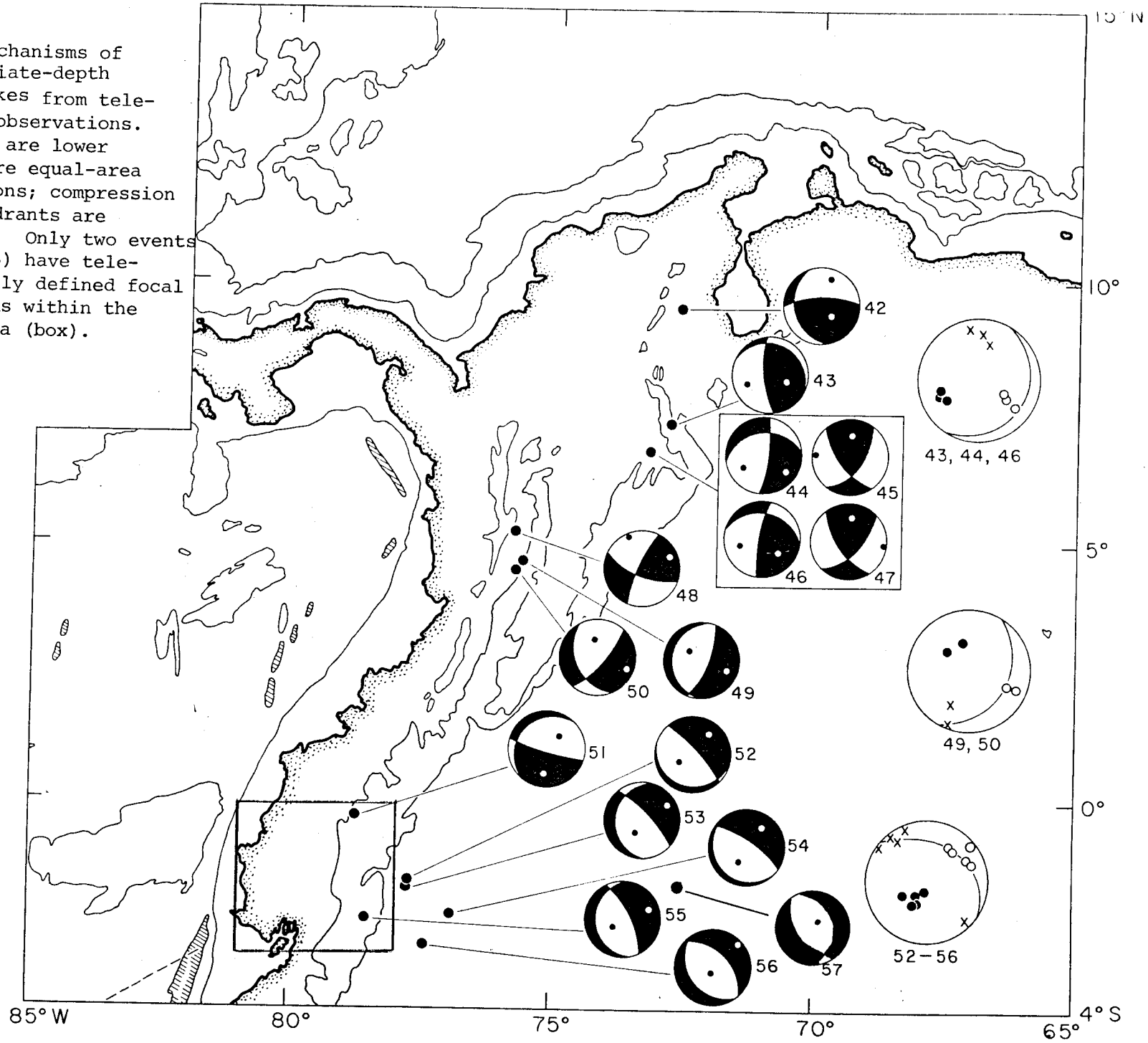

Fig. 1G.
Focal mechanisms of intermediate-depth earthquakes from teleseismic observations. Diagrams are lower hemisphere equal-area projections; compression wave quadrants are darkened. Only two events (#51 & 55) have teleseismically defined focal mechanisms within the study area (box).

Fig. 1H.
Teleseismically well-determined shallow-focus epicenters. Larger symbols are better locations. Seismicity in the study area (box) is diffuse.

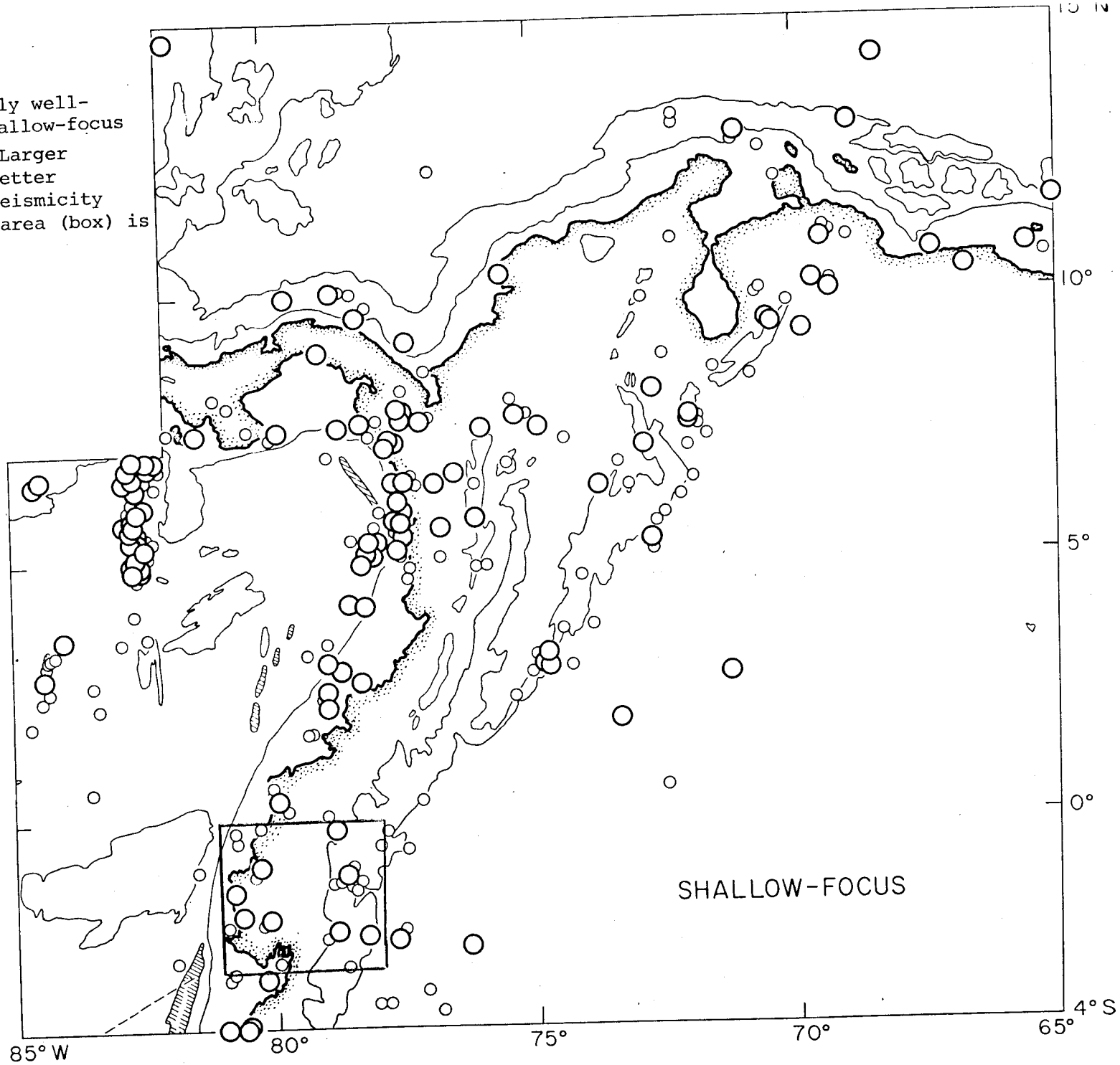

Figure 1I. Focal mechanisms of shallow-focus earthquakes. Diagrams are lower hemisphere, equal-area plots; compressional-wave quadrants are darkened. Tension and pressure axes are white and black circles, respectively. Only one teleseismically defined focal mechanism is known for the study area (#28). This event shows thrusting in response to E-W compression.

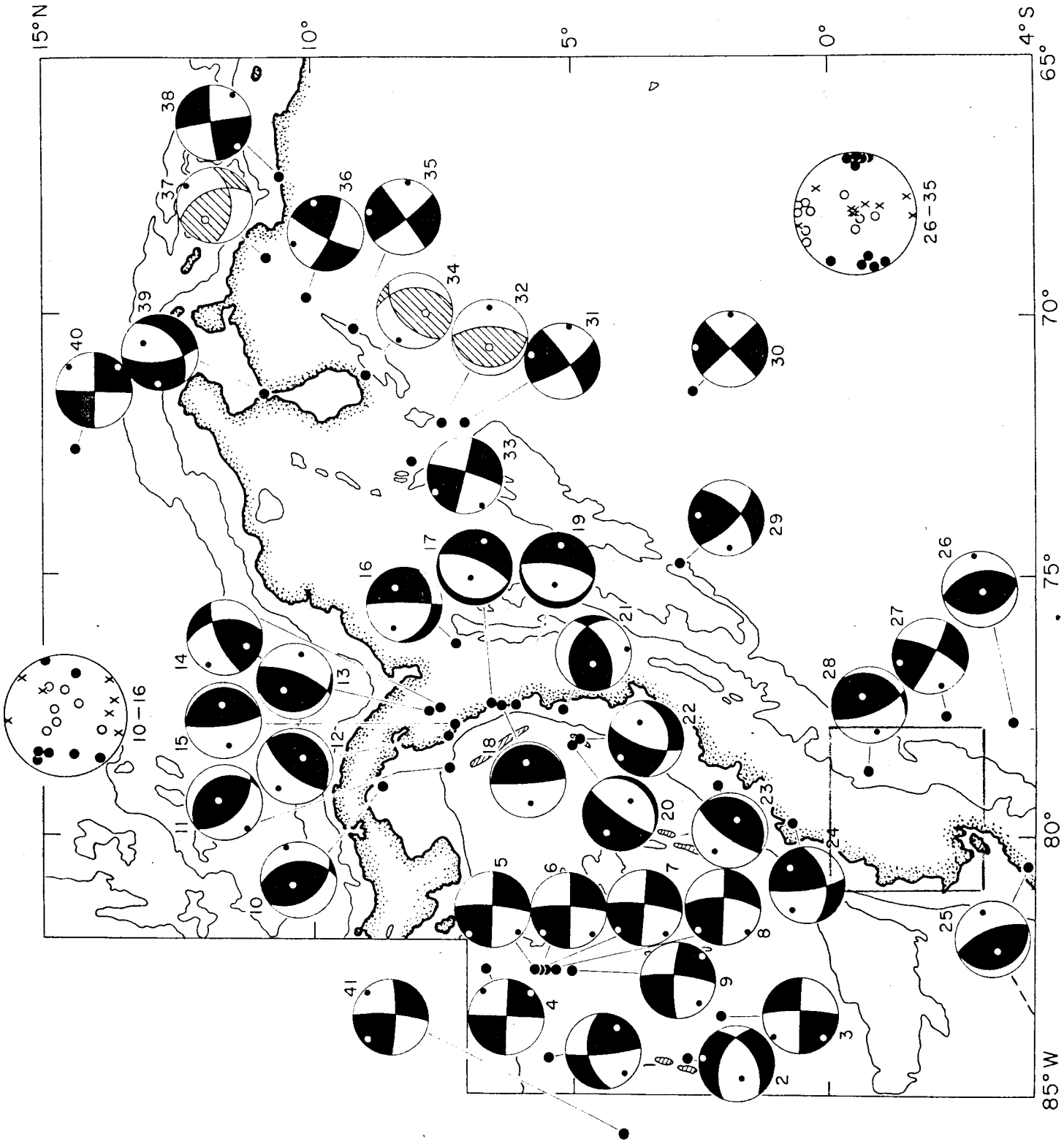

Fig. 1J. Identification of the "Audean Block." The southern terminus of the eastern Audean Frontal Fault Zone is not well-defined; it may be the Gulf of Guayaquil, after cutting across the Andes in the study area (box) along several faults.

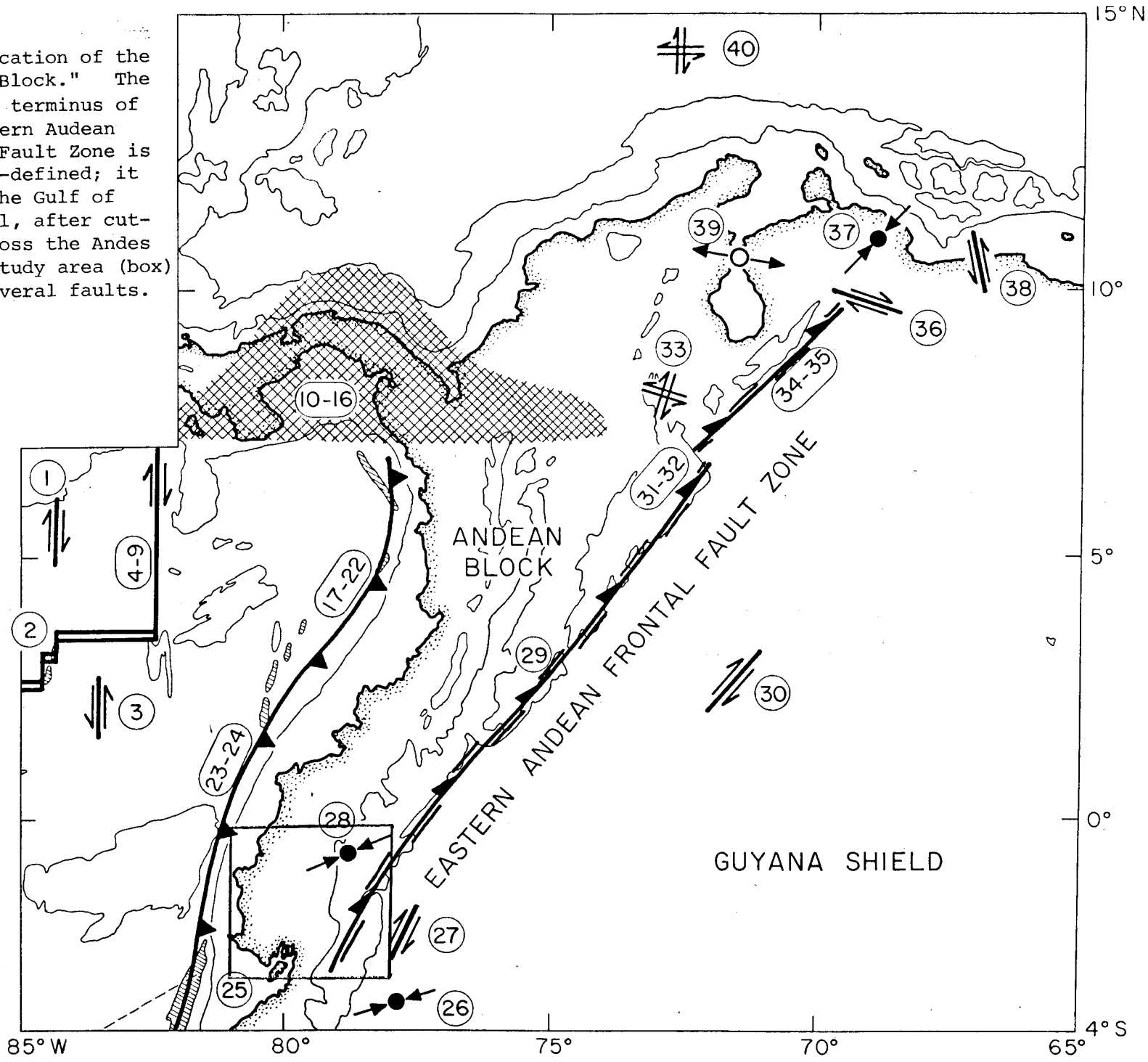

Nazca plate in the west and the South American plate in the east. The presence of the seismic Benioff zone is well established through the investigations of the distribution of earthquake hypocenters and focal mechanism studies along the continental margin. This is the only major subduction zone where an oceanic slab descends under a continent. This area accounts for about 15% of the world's seismic activity. The present day seismicity, however, is by no means uniform through this area. There are marked north-south variations in the presence of deep earthquakes which are confined to rather narrow latitudinal zones. Similarly, there is a conspicuous absence of intermediate depth earthquakes between about 320 and 525 km along the entire margin. The active volcanism associated with the Andes is also largely variable, with the main activity concentrated in southern (32° - 43°S) and northern Chile and in southern Peru, Ecuador, and Colombia.

There are several features in the seismicity in South America which are different from those in other pure island-arc systems. The value of b in Gutenberg-Richter's formula $\log N = a + b(8 - M)$, for instance, is 0.4 - 0.5 in South America, which is significantly lower than the values in any other island arc regions (Santo, 1969). Epicenters of the upper mantle earthquakes shallower than 200 km crowd in several small areas, forming "nests". The most prominent nest is the "Bucaramanga" nest and is located at about 6.8°N, 73.0W in northern Colombia (Pennington, et al., 1979). Another prominent one is located at about 1.3°S,77.8°W beneath the central portion of Ecuador. Absence of seismic activity between depths of 320 and 525 km is another characteristic in this area. Earthquakes deeper than 550 km originate along two separate arcs with the length of approximately 1000 km in each, one located along the eastern border of

Peru and another along northwestern Argentina. They are characterized by releasing a large amount of energy in spite of their few occurrences. The energy released by the deep earthquakes of 600 - 640 km, for instance, accounts for about 30% of the total energy in this area, which is equivalent to the energy released by whole crustal earthquakes. There is considerable seismic activity within the upper 50 km of the overriding South American plate. This seismic activity is well separated from the inclined seismic zones and probably occurs in the crustal part of the South American plate. Although the shallow seismic activity is relatively dispersed most of the activity is near the eastern flanks (sub-Andean zone) of the Andes regardless of the distance of the sub-Andean zone from the trench.

2.2 Seismicity in Ecuador

Ecuador lies along the very seismically active continental margin covering from about 1.5°N to 5°S and has experienced numerous earthquakes of strong intensity. Epicenters of shallow earthquakes lie in two principal belts; one follows the Dolores-Guayaquil megashear, and the other lies offshore. As elsewhere in the Andean chain, the hypocenters lie at progressively greater depths toward the east, being related to subduction zones: the offshore belt has shallow epicenters (h: <70 km), whereas those in the Andes are of moderate depth (h: 130-180 km). Deep-seated earthquakes (h: 550-650 km) have been recorded from the western Guayana Shield beyond the Ecuador frontier (Fig. 2A).

In and near Ecuador, there are several areas of heavy concentration of epicenters; two of shallow earthquakes and one of intermediate-depth earthquakes. One concentration of shallow earthquakes is located at about 4.1°S, 80.9°W, approximately 200-250 km southwest of Guayquil and the other at

60001-81058

FIG. 2A

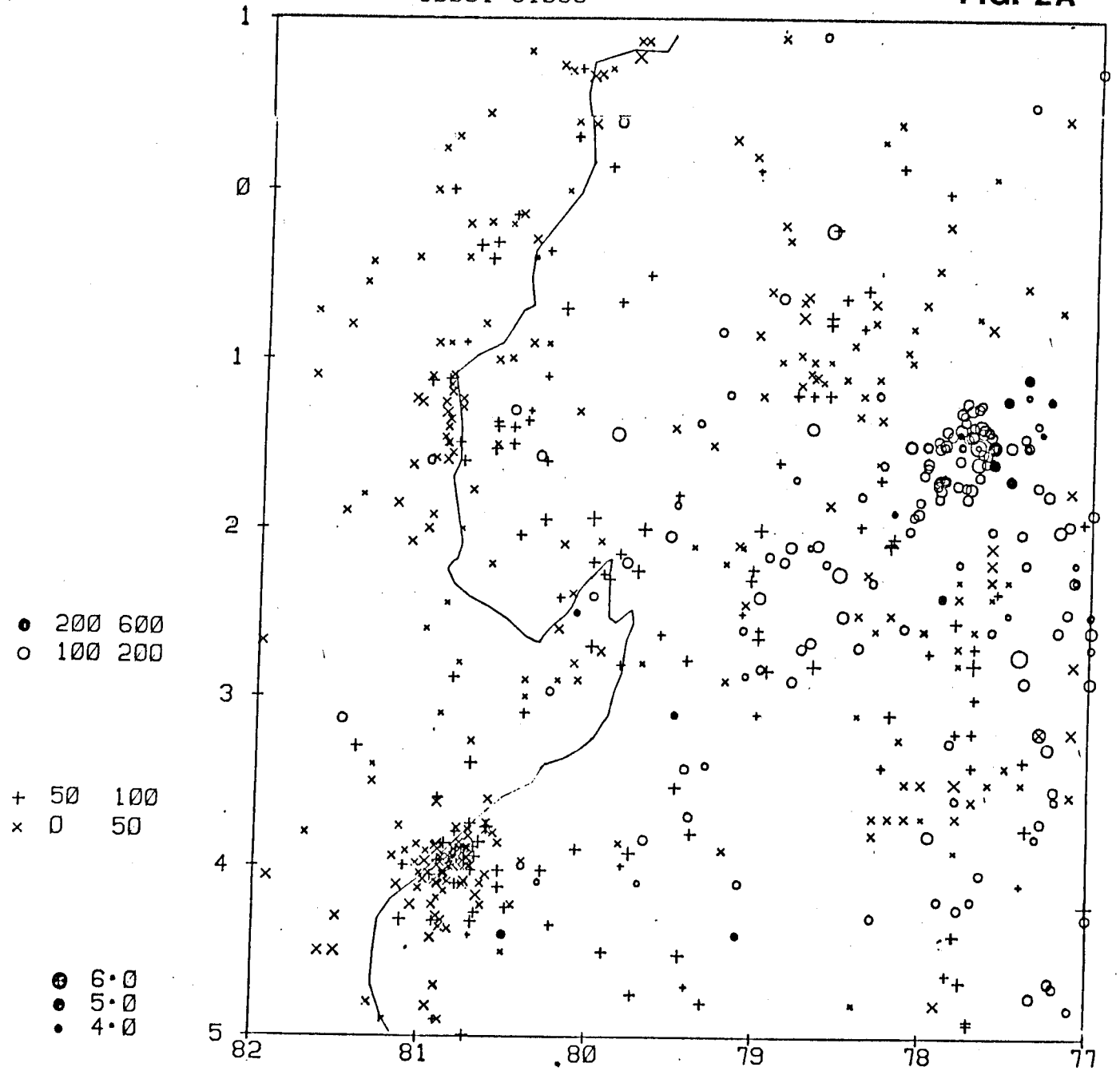

about 5.5°S, 77.1°W, approximately 250-300 km southwest of Gualaquiza. That of intermediate-depth earthquakes is located at about 1.3°N, 77.8°W, approximately 170-230 km northeast of Cuenca (see Fig. 1C and 1E). These three areas are very important and should be carefully monitored for seismic risk study in Ecuador.

An extensive activity in and near the Galapagos Islands is shown in Figure 2B. The majority of earthquakes were attributed during 1968 in association with 1968 Fernandina Caldera Collapse. Of 343 events shown in Figure 2, 260 earthquakes were reported in 1968. No earthquakes deeper than 50 km were reported in the area in Figure 2B.

2.3 Historical Earthquakes and Earthquake Prediction in Ecuador

The list of historical earthquakes (Table 1) shows that Ecuador has experienced a number of earthquakes of very large magnitude. In 1906 an extremely large, shallow earthquake (M = 8.9) accompanied by a large tsunami occurred off the Ecuador Colombia coast. The Ambato earthquake of 1949 cost about 6000 lives. This table shows the importance of seismic risk study in Ecuador since Ecuador has been frequently subject to large earthquakes historically.

A crude method to predict locations of large shallow earthquakes of the near future along major plate boundaries is developed based on the past space-time pattern of occurrence of large earthquakes, the lateral extent of their rupture zones, and the direction of rupture propagation. The lateral extent of the rupture zones of large shallow earthquakes is determined by mapping the distribution of aftershocks, coastal deformation, and seismic intensity. From such maps, it is possible to identify segments of the siesmic belts that have not experienced large earthquakes for many

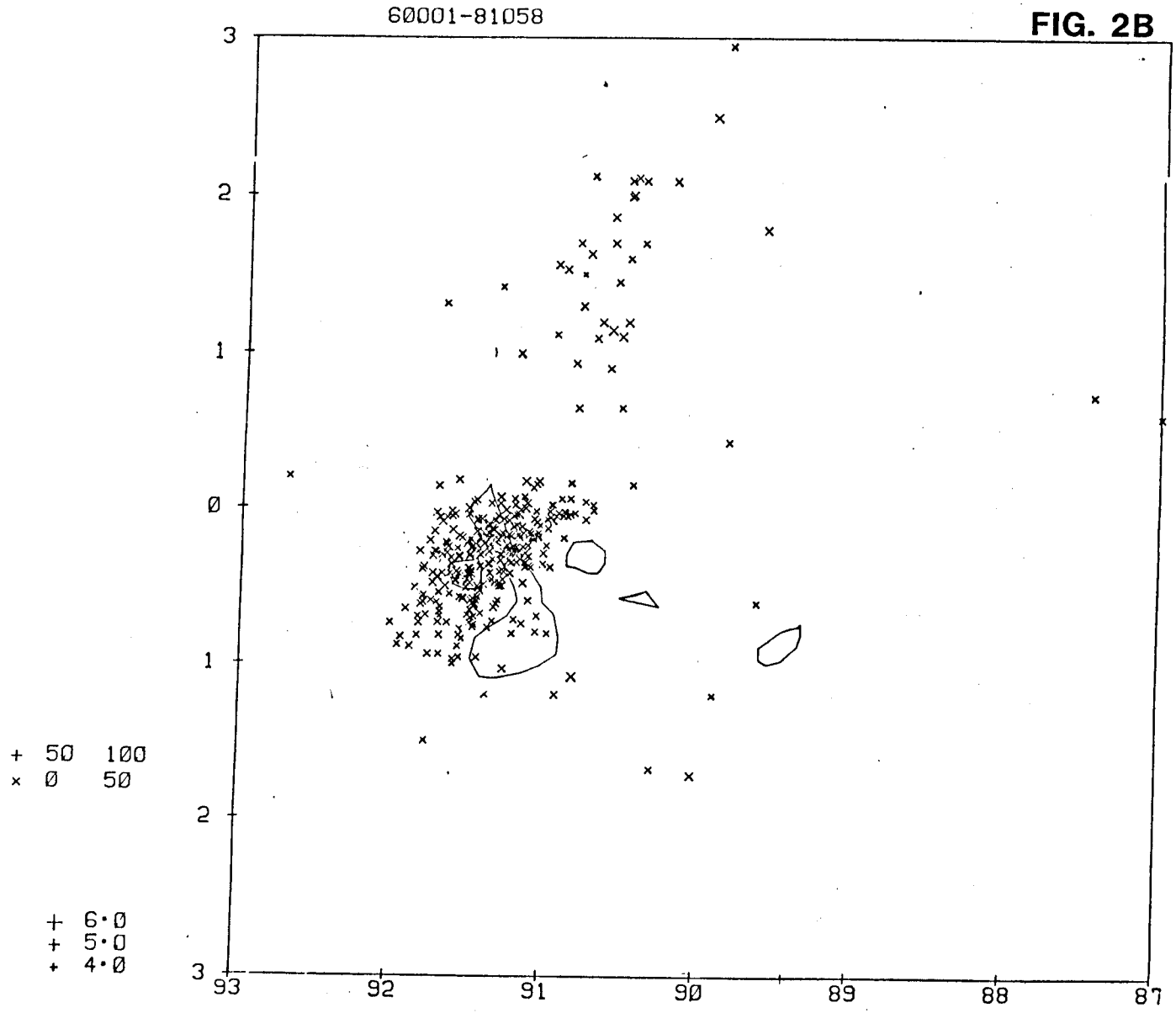

FIG. 2B

Table 1. Historical Earthquakes In and Around Ecuador*

No.	Date	Epicenter	M	Comments
1	1587 Aug. 30	Quito, Ecuador		
2	1698 Jun. 19	Ambato, Ecuador		
3	1735 Feb. 2	Popayan, Colombia		
4	1755 Apr. 26	Quito, Ecuador		
5	1757 Feb. 22	Latacunga, Ecuador		
6	1797 Feb. 4	Ambato, Ecuador		
7	1827 Nov. 16	Popayan, Colombia		
8	1834 Jan. 20	Pasto, Colombia		
9	1859 Mar. 22	Quito, Ecuador		
10	1868 Aug. 16	Ibarra, Ecuador		
11	1885 May 25	Popayan, Colombia		
12	1887 Aug. 2	Cuenca, Ecuador		
13	1901 Jun. 7	Guayaquil, Ecuador		
14	1906 Jan. 31	Off north Ecuador	8.9	Tsunami
15	1935 Aug. 7	Pasto, Colombia	7.5	
16	1942 May 14	Off Ecuador	8.3	
17	1947 Jul. 14	Pasto, Colombia		
18	1949 Aug. 5	Ambato, Ecuador	6.8	6,000 dead
19	1958 Jan. 19	Colombia-Ecuador	7.8	

* Data from Lomnitz (1974)

decades. Such quiescent sites appear to be zones of relatively high seismic risk for the near future, particularly if major shallow earthquakes are characteristic of the zone. Some studies along circum-Pacific seismic zones (Fedotov, 1965; Mogi, 1968) indicate that such gaps between rupture zones tend to be filled eventually by large-magnitude earthquakes.

Kelleher (1972) and Kelleher et al. (1973) attempted to forecast likely locations for large shallow earthquakes in the shallow seismic zone of western South America by the above mentioned. An advantage of studying the South American seismic zone lies in the fact that single lithospheric plate extends from 46°S to at least 4°N. There are no triple points or bifurcations of the seismic zone within these limits. Thus the effect of great earthquakes on adjacent sections of the plate boundary should be discernible here if anywhere. They defined five seismic gaps along western South America: Central Chile (33° - 35°S), northern Chile-southernmost Peru (about 17° - 25°S), South of Lima (about 12.5° - 14°S), northern Peru-southern Ecuador (about 9° - 1°S), and northern Ecuador-southern Colombia (about 2° - 4°N). The last two gaps, i.e., northern Peru-southern Ecuador and northern Ecuador-southern Colombia, are essentially important to the seismic risk study in Ecuador because these gaps are very close to the land of Ecuador. The last gap listed has recently experienced a large earthquake (Dec. 1979) and is not considered a gap at the present time. There is reason to suspect that the gap near 1°S is permanent, being associated with the subduction of the Carnegie ridge (Kellcher and McCann, 1976; Pennington, 1981, 1983, in press).

3. DAULE-PERIPA SEISMOGRAPH NETWORK

3.1 Establishment and operation of the Daule-Peripa Seismograph Network

Immediately after the contract was signed by the University of Texas on July 28, 1981, UT scientist started to explore the location of the remote sites. Dr. Matumoto visited Ecuador twice in 1981 and selected the location of the remote sites (Field Reports on the site selection were submitted on October 12 and November 23, 1981, respectively).

The procurement, assembly, and adjustment of the equipment for the network progressed on schedule and the equipment for the seismic system was ready by the end of 1981. Due to the delay in importation permit, however, the equipment was held in Texas at the request of CEDEGE and was finally shipped to Ecuador in early April, 1982. During April, the technical crew from the University worked with the supporting group from CEDEGE to establish the network. With 3 weeks of long, hard field work (10 to 14 hours of daily work, including weekends and holidays) the network was established and started its first operation on April 23, 1982. Table 2 and Figure 3A show the location of the stations.

After 12 hours of operation, however, the system started to develop some problems. The cause of the problems was located on the computer boards, which were damaged from mechanical stress such as severe flexing or impact. This damage, it was suspected, may have been caused at the time when the computer was hand carried in the CEDEGE building (see Field Report, April 19, 1982).

At the time of construction, difficulties in the data transmission from some of the remote stations was experienced. Some of the problems were attributed to malfunctioning equipment and most of the problems related to

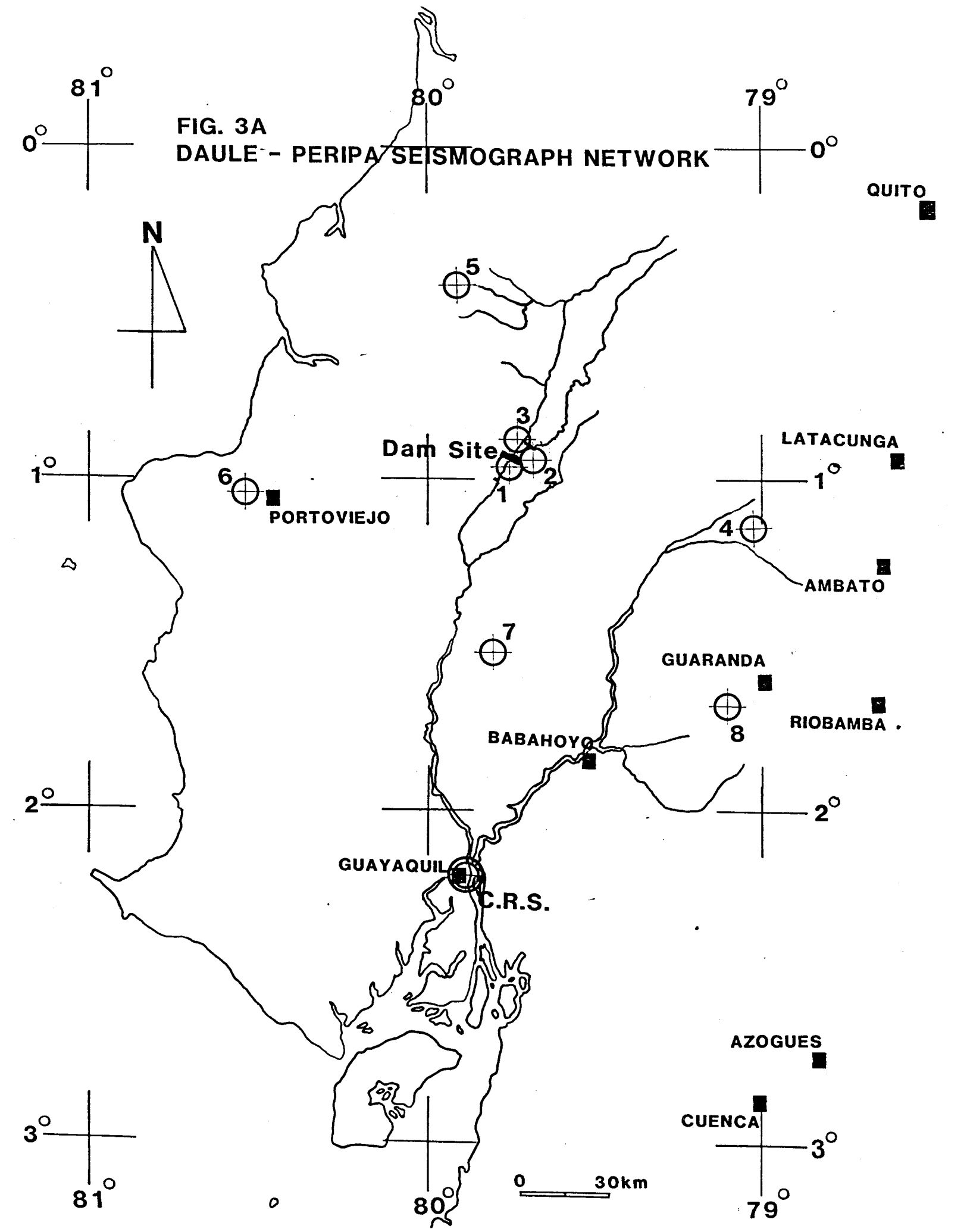
FIG. 3A
DAULE - PERIPA SEISMOGRAPH NETWORK
81°
80°
79°
0°
1°
2°
3°
N
QUITO
LATACUNGA
AMBATO
GUARANDA
RIOBAMBA
BABAHOYO
PORTOVIEJO
Dam Site
1
2
3
4
5
6
7
8
GUAYAQUIL
C.R.S.
AZOGUES
CUENCA
0
30km

October 13, 1982

TABLE 2

DAULE-PERIPA SEISMIC NETWORK (ECUADOR)

STA #	STA NAME	MAP NAME	MAP #	ELEV.(m)	DISTANCE TO CRS(KM)	LAT.(S)	LONG.(w)	MAP COORDINATE Y (km)	MAP COORDINATE X (km)
Dam Site		Techel	N III E3	30	141.5	0.92075	79.75089	0	0
CRS		Guayaquil	N V A 3	5	0	2.19294	79.87928	-140.83	-14.21
1		Tachel	N III E 3	122	137.9	0.95333	79.75178	-3.61	-0.10
2		Guayas	N III E 4	126	139.9	0.94456	79.68408	-2.64	7.40
3		Guayas	N III E 4	120	147.4	0.86981	79.73003	5.64	2.31
4		El Corazon	N IV B 2	2369	149.8	1.14381	79.02406	-24.69	80.46
5		Flavio Alfaro	N III C 1	276	196.6	0.41689	79.90536	55.78	-17.10
6		Montecristi	M IV A 2	680	146.7	1.04464	80.54153	-13.71	-87.52
7		Palestina	N IV C 3	35	74.9	1.52081	79.80475	-66.43	-5.96
8		San Miguel	N IV F 2	2620	103.0	1.67794	79.10444	-83.82	71.56

the equipment was corrected by the end of May 1982. The RF link from two stations (stations 4 and 6), however, were found to be inadequate due to selection of the remote stations (monthly report, June 1982). Station 6 was situated adjacent to a high power line a and the line of sight for data transmission was obscured by a utility tower, reducing the RF power significantly. The antenna tower at station 6 was finally relocated by the CEDEGE crew in the middle of September 1982.

The site of station 4, moved from the original selection to the new site selected by CEDEGE for logistic reasons, was found to be inadequate for the requirement of the line of site. Recommendation for relocation of station 4 was issued on several occasions (letter to Mr. Eade, July 23, 1982; letter to Ing. Dominguez, July 23, 1982; field report August 21, 1982), but these recommendations were not adopted. As an alternative solution, rerouting of the data path was proposed (st. 4 - st. 1 - st. 8 - Central recording station). This change of data transmission path was realized by Donald McGhee in April 1983.

In the middle of September 1982, intermittent malfunctions of the Versatec printer/plotter was reported. On October 24, it finally became non-operative. At our request, the printer/plotter was shipped back to Texas for repair but it suffered even greater mechanical damages during transportation due to poorly handled packing. Nevertheless, the printer/plotter was repaired (power supply was malfunctioning) and sent back to Ecuador on November 16, 1982. This equipment, however, was held at the customs warehouse until late January 1983.

Immediately after reinstallation of the printer/plotter, an additional malfunction of TTY was uncovered. After unsuccessful attempts to repair the troubled TTY by the local repairman, we requested the travel authorization

for our technician to visit Ecuador on 9 March 1983, which was granted on 29 March 1983.

Subsequently, Donald McGhee, technical engineer of the University of Texas, took off on 8 April 1983. He cured all the problems and recalibrated the system. The network resumed its normal operation on 11 April 1982 (Field Report 9 May 1983).

During the operating period from 24 May 1982 through 24 October 1982, 287 events were recorded. An additional COSMOS data covering 11 April 1983 through 30 May 1983 was received by the University on 21 June 1983.

3.2 Design of the Network

3.2.1 Remote Stations

Figure 3B shows the schematic diagram of the CEDEGE seismograph network. At a remote station, small ground movement is converted to electric signal by a geophone, amplified and modulated by a PA/VCO and then transmitted by VHF radio frequency transmitter to the central recording station. The site of a remote station is usually chosen on the considerations of (1) the optimum distribution for detection of earthquakes, (Sato and Skoko, 1965), (2) low noise, and (3) line of sight to the central recording station. If a station has no direct line of sight back to the central recording station, the signal has to be transmitted to the repeater station and then retransmitted to the central recording station. At the repeater station, as needed, signals of up to eight stations can be mixed together (multiplexed) and transmitted to the central recording station by a single radio transmitter. Each multiplexed station needs to be modulated by the different frequency to avoid the interference from other stations. The multiplexer usually includes filter cards for each channel, a summing

CEDEGE Seismograph Network

FIG. 3B

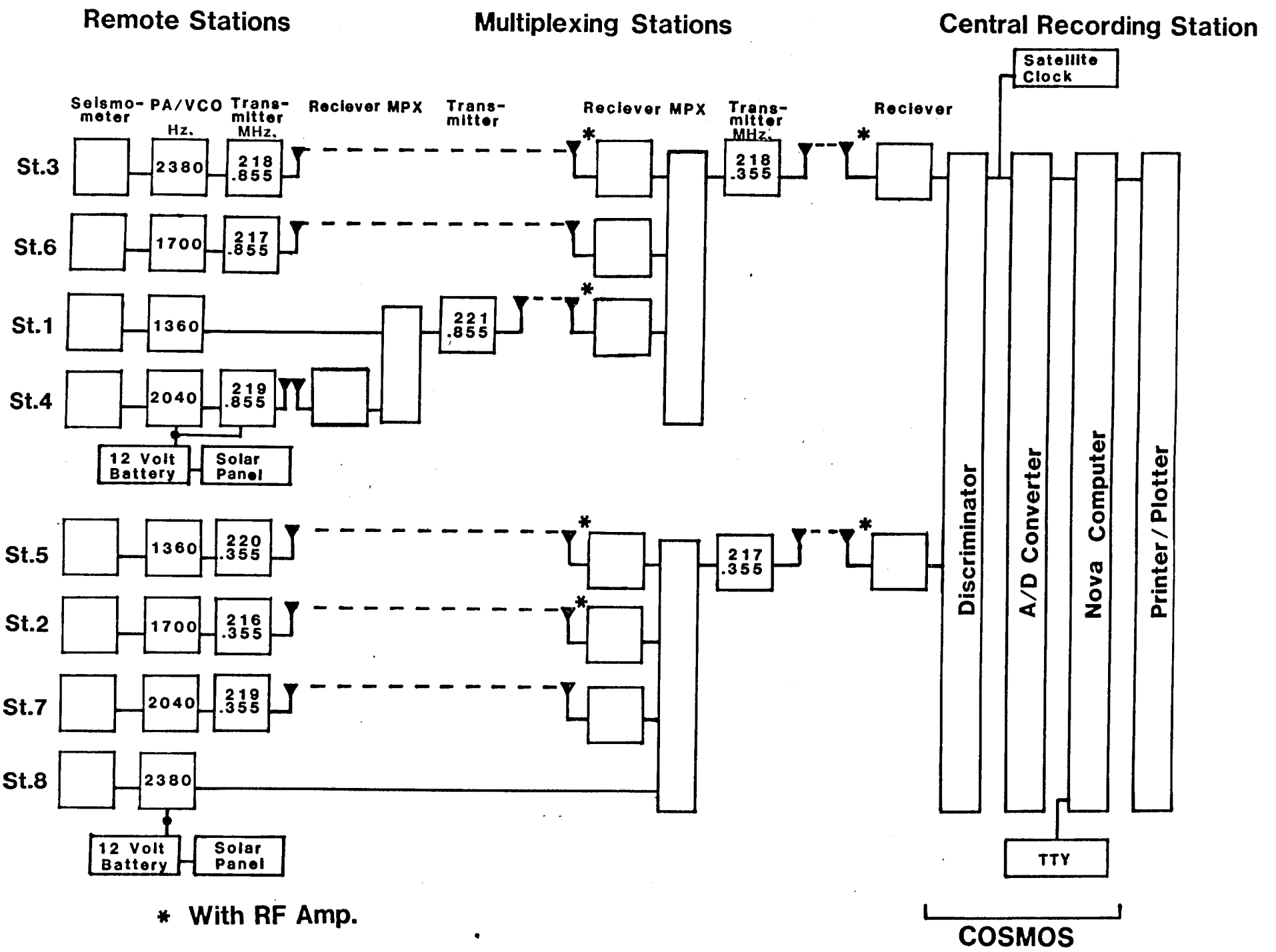

amplifier, and power supply unit. A filter card is featured by a sharp band pass (VCO center frequency I 125 Hz) with 24 db roll off to prevent cross talk back to the adjacent data channels. The power for remote/ multiplexed stations is supplied from 12-volt battery and charged by solar panels.

3.2.2 Central Recording Station

Upon reaching the central recording station, the signal is received by a receiver and then demodulated by a discriminator with matching frequency and fed into the Computerized Seismic Monitoring System (COSMOS). Figure 3C shows the logic flow chart of COSMOS. Here possible earthquakes are detected through a triggering logic and are plotted onto a high-speed printer/plotter. COSMOS initiates the automatic epicenter determination program when four or more stations are set on "trigger" mode and the arrival times for P-waves, COSMOS computes a preliminary location of an earthquake without human assistance. Within COSMOS software, which was written in the Real-Time Disk Operating System, the epicenter program is concurrently executed, but this epicenter determination program occupies the central processing unit only when the high-priority data scanning monitoring program is completed and the computer becomes idle before the next sampling cycle starts. In this way, the epicenter is calculated without disturbing the main program that continues to monitor the incoming seismic signals. This automatic epicenter determination is one of the powerful features that play an important role in the real-time seismic monitoring program, which locates the epicenter, depth, and the magnitude of an earthquake and prints them out immediately. At the time of impounding a reservoir which frequently triggers a number of water-induced earthquakes, such an automatic epicenter determination capability becomes very important.

FIG. 3C

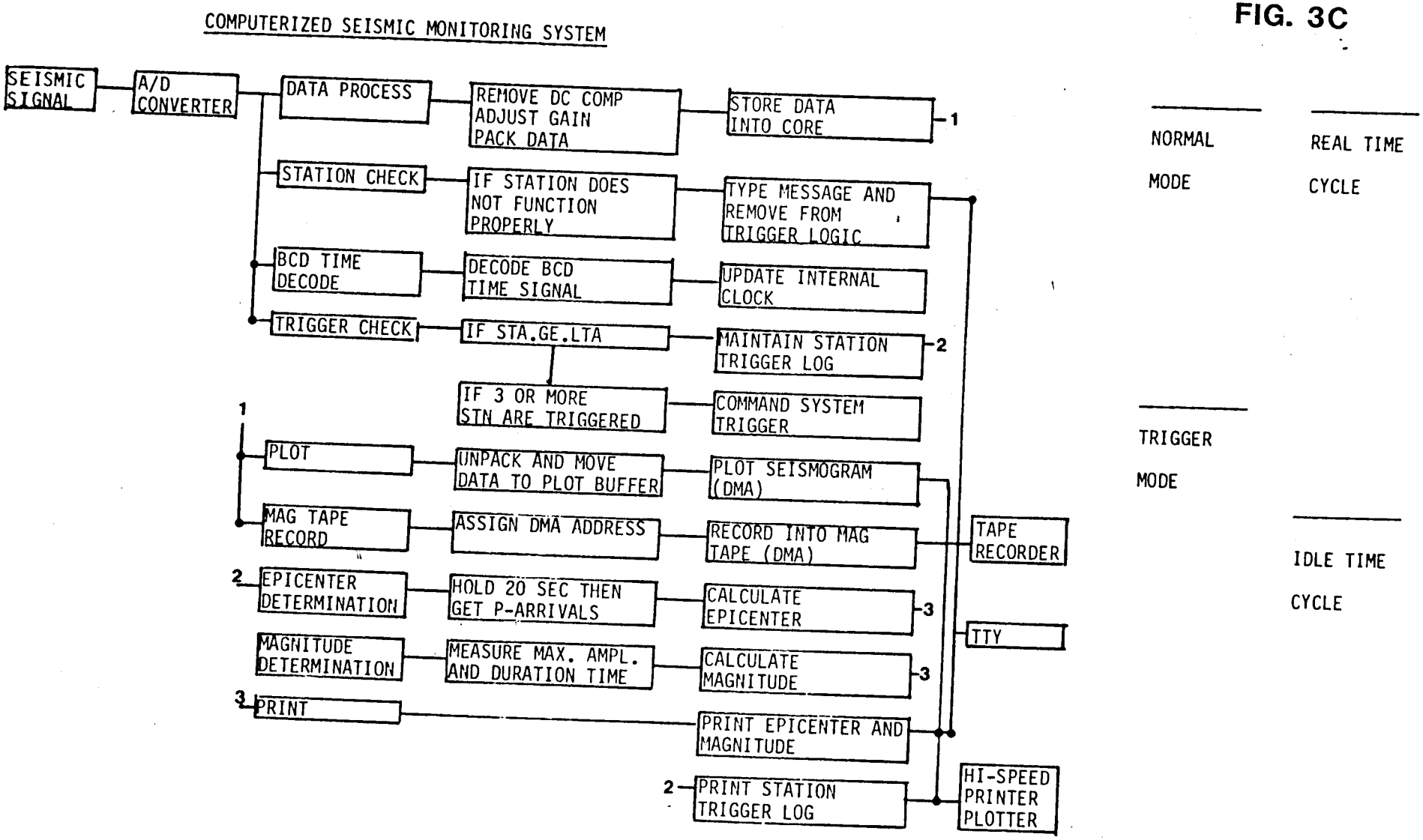
COMPUTERIZED SEISMIC MONITORING SYSTEM
SEISMIC SIGNAL
A/D CONVERTER
DATA PROCESS
REMOVE DC COMP ADJUST GAIN PACK DATA
STORE DATA INTO CORE
1
STATION CHECK
IF STATION DOES NOT FUNCTION PROPERLY
TYPE MESSAGE AND REMOVE FROM TRIGGER LOGIC
BCD TIME DECODE
DECODE BCD TIME SIGNAL
UPDATE INTERNAL CLOCK
TRIGGER CHECK
IF STA.GE.LTA
MAINTAIN STATION TRIGGER LOG
2
IF 3 OR MORE STN ARE TRIGGERED
COMMAND SYSTEM TRIGGER
1
PLOT
UNPACK AND MOVE DATA TO PLOT BUFFER
PLOT SEISMOGRAM (DMA)
MAG TAPE RECORD
ASSIGN DMA ADDRESS
RECORD INTO MAG TAPE (DMA)
TAPE RECORDER
2
EPICENTER DETERMINATION
HOLD 20 SEC THEN GET P-ARRIVALS
CALCULATE EPICENTER
3
TTY
MAGNITUDE DETERMINATION
MEASURE MAX. AMPL. AND DURATION TIME
CALCULATE MAGNITUDE
3
3
PRINT
PRINT EPICENTER AND MAGNITUDE
2
PRINT STATION TRIGGER LOG
HI-SPEED PRINTER PLOTTER
NORMAL MODE
REAL TIME CYCLE
TRIGGER MODE
IDLE TIME CYCLE

While this automatic epicenter determination is an important tool for the real-time seismic monitoring program, the users of this system should bear in their minds that there are some limitations due to the structure of the computer program. The limited capability of the automatic epicenter determination in COSMOS is attributed from the following reasons:

(1) the computer program is able to identify P-way only; no S-wave is identified and utilized in the epicenter determination process;

(2) in the computer program, the onset of "P-wave" is identified as the time when the input signal exceeds the threshold determined by the background noise. Therefore, if the onset of the signal is quite slow (as usually expected for distant earthquakes) or during the time period with noisy background (as experienced on windy weather or with animal noise), the identified "P-arrival" does not necessarily represent the true onset, actually such a mistrigger is rather common;

(3) there is a tendency that the computer identified P-arrivals are the arrival time of the peak amplitude rather than the beginning of an onset. Accordingly, the computer identifying P-arrivals usually lags approximately 0.5 to 0.1 seconds behind the actual onset time (approximately 1/4 of the predominant period).

Due to these effects, the epicenter located by the automatic program is reasonably reliable only when:

(1) the signals are detected by more than 5 stations,

(2) the signals have sufficient S/N ratio (at least 10:1), and

(3) the earthquake is situated within the network and characterized by the high frequency onset.

Table 3. Comparison of Epicenter Determined By COSMOS Program and Conventional Method

Class	*Error KM	No. of Events	No. of events that include misidentified onset by COSMOS
AA	less than 2 km	7	
A	2 km≤E<10 km	15	
B	10 km≤E<20 km	4	1
C	20 km≤E<50 km	21	19
D	More than 50 km	45	45

*Error indicates the difference between two epicenter determinations

Table 3 shows the comparison of the foci determined by COSMOS automatic program and the conventional, eye-ball analysis. Of 92 selected events compared, (recorded by the network of Dominican Republic during the period from January through December, 1980) only 22 events (in class AA and A) are sufficiently close to each other. The majority of these events are generated by the explosion, for which the onset of P-arrivals is usually large and sharp. On the other hand, the number of events in class C and D, that are considered to be erroneous determination, amounts to 66, three times as many as the number of the events in classes AA and A combined. Most of these events are either events that occurred at greater distances and/or those registered with small and gradual onset. At least one misidentified reading, which is responsible for large error, was involved in the automatic epicenter determination and is significantly different from the result of the eye-ball analysis. Therefore, the results from the automatic epicenter determination should be regarded as a preliminary estimate. If the preliminary results are to be utilized for more detailed analysis, it is necessary to determine whether any errors are involved in the identification of the onset.

The revised program effective March 3, 1981, includes the function to examine and to eliminate a false identification of the arrival times. This revision automatically eliminates the readings that do not match the logical acceptable pattern of the arrival times. It is expected that an improvement of the automatic epicenter determination will be significant.

3.2.3 Example of a Seismograph

Figure 3C shows the sample of the CEDEGE network. The signals from 8 stations (station 4 was not in adjustment at the time of this recording)

FIG. 3C

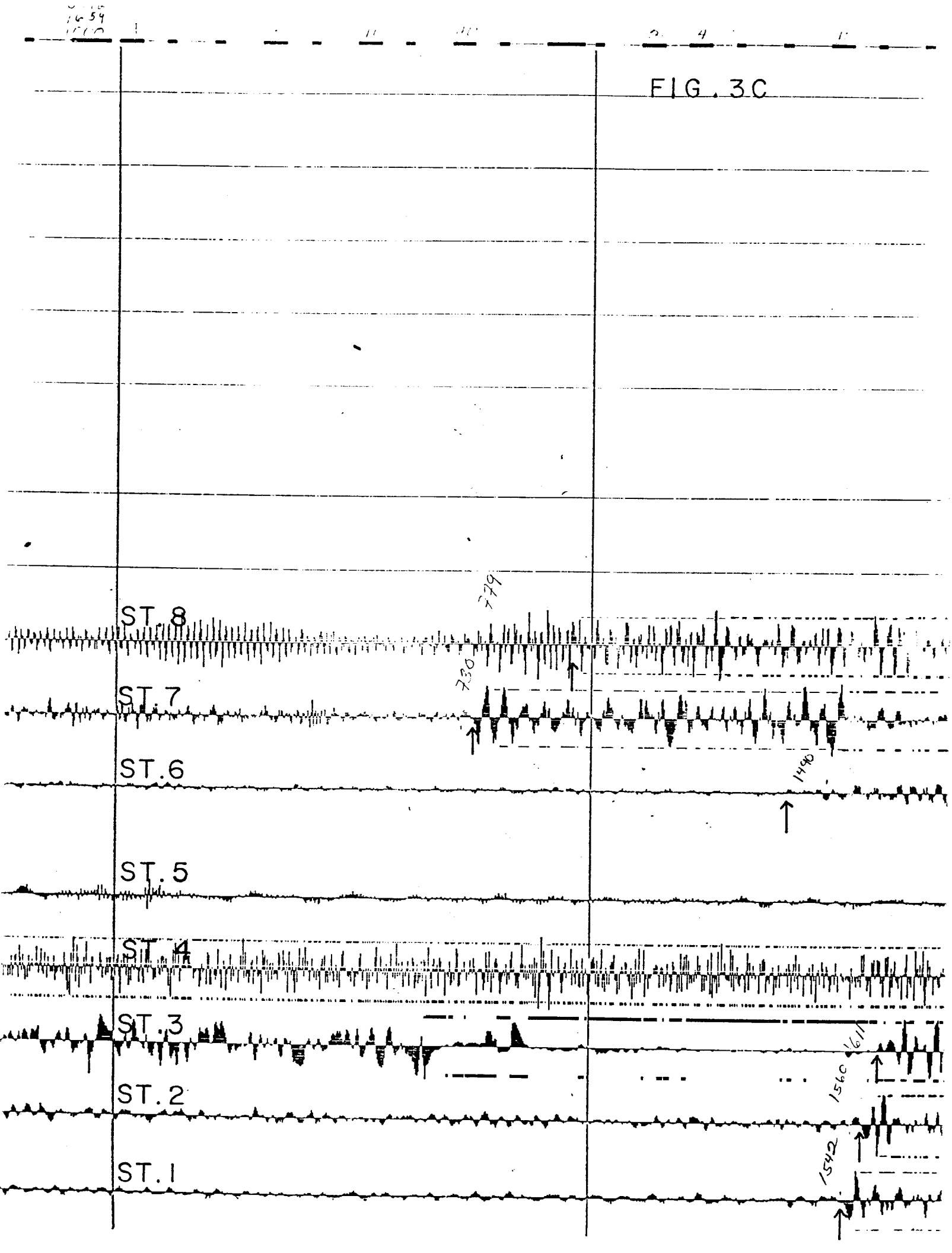

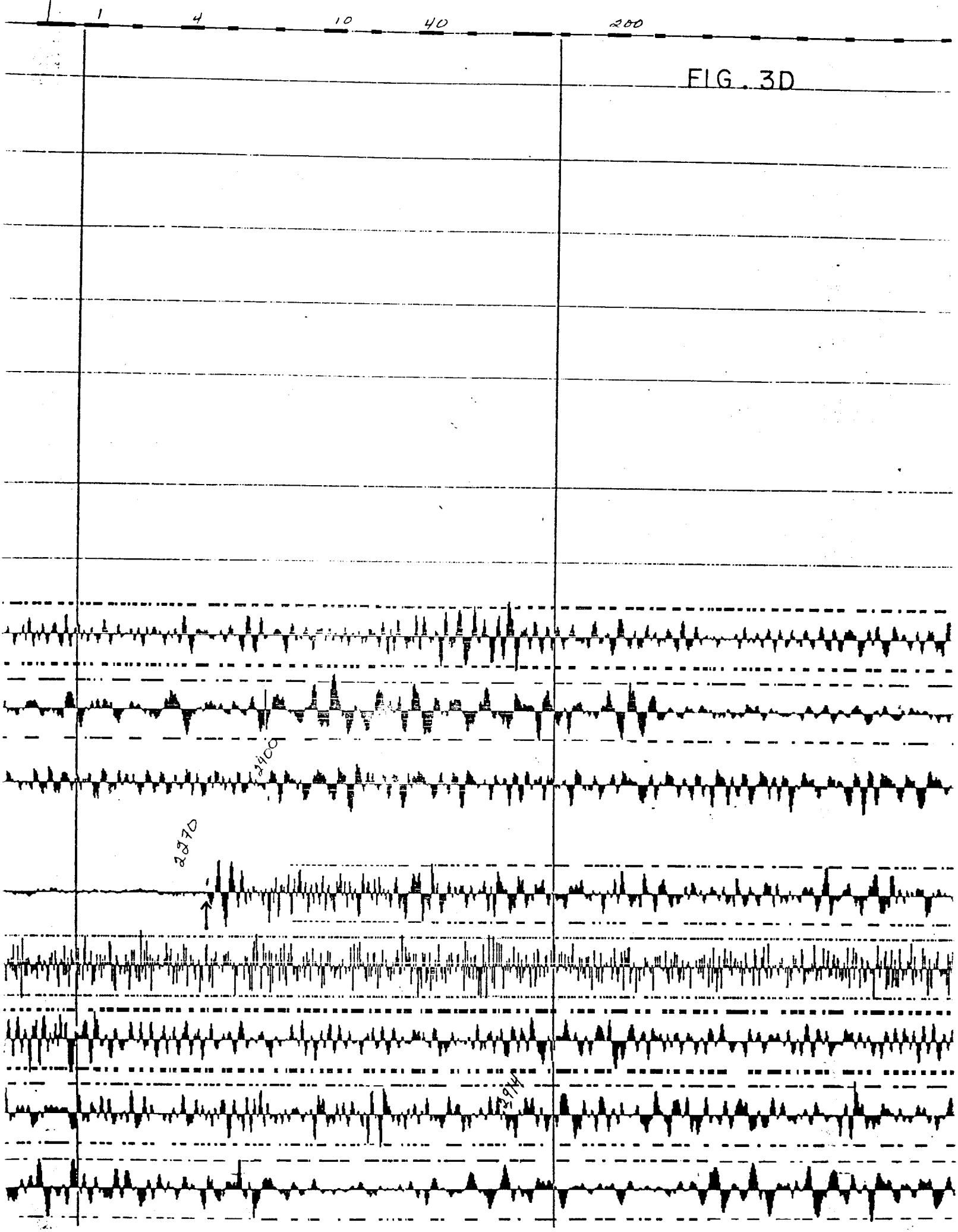

FIG. 3D

FIG. 3E

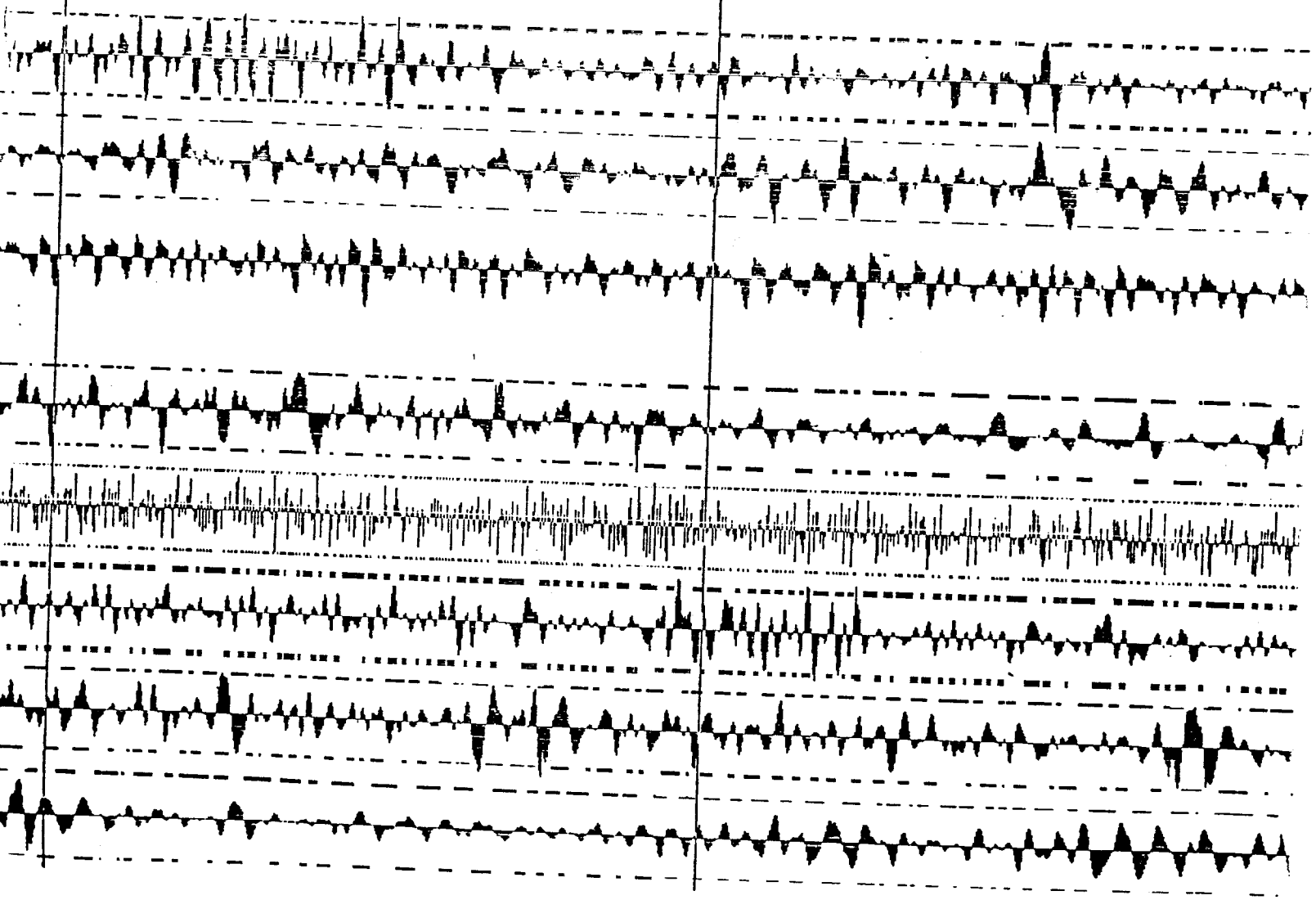

CEDEGE NETWORK ECUADOR

FIG.3F

INPUT DATA

YR	DAY	H	M	S	NP	ITER	MB
82	255	16	59	17.21	4	10	3.4

ST NO	1	2	3	4	5	6	7	8	9	10	11	12	13	14	15
TP	8.18	8.73	0.00	0.00	0.00	0.00	-0.07	5.15	0.00	0.00	0.00	0.00	0.00	0.00	0.00
TPOC	-0.04	0.04	0.00	0.00	0.00	0.00	0.00	0.00	0.00	0.00	0.00	0.00	0.00	0.00	0.00
U/D	0	0	-1	0	0	0	0	-1	0	0	0	0	0	0	0
DIST(KM)	226.72	230.46	235.42	251.10	278.16	200.91	167.19	203.19	0.00	0.00	0.00	0.00	0.00	0.00	0.00
MxAMP(MV)	82	102	348	0	62	110	135	384	0	0	0	0	0	0	0
MS	3.26	3.38	0.00	0.00	0.00	0.00	3.03	4.02	0.00	0.00	0.00	0.00	0.00	0.00	0.00
TP-T0	8.18	8.73	0.00	0.00	0.00	0.00	-0.07	5.15	0.00	0.00	0.00	0.00	0.00	0.00	0.00

ORIGIN TIME
82 255 16 58 51.17

EPICENTER	LONG(DEG)	LAT(DEG)
	-80.4994	-2.8576
REF. PT. FOR X,Y	-79.7509	-0.9208

	OT	X(KM)	Y(KM)	Z(KM)	DS	S
	-26.04	-81.95	-214.23	10.81		
ST. DIV.	0.31	1.83	1.92	0.30		0.05

ITERATION

1	-11.91	-15.03	-57.01	10.31	0.00	2.72
2	-23.70	-72.60	-128.51	10.31	91.85	0.58
3	-24.96	-74.02	-139.14	10.31	10.71	0.30
4	-25.59	-74.79	-144.54	10.31	5.41	0.13
5	-25.82	-75.19	-146.22	10.31	1.91	0.08
6	-25.93	-75.64	-147.07	10.31	0.96	0.06
7	-25.99	-75.86	-147.39	10.31	0.48	0.06
8	-26.02	-75.97	-147.70	10.31	0.24	0.06
9	-26.04	-76.03	-147.81	10.31	0.12	0.05
10	-26.04	-76.05	-147.86	10.31	0.06	0.05

and the Binary Coded Time Signal are shown in this figure. A vertical reference line is drawn each 10 seconds. When an earthquake is detected, the COSMOS system starts to plot the seismic signals. Because of the delay time programmed in the system, the onsets of the seismic signal start to appear approximately 20 seconds after the system is triggered. When the amplitude of the signal exceeds the plotting threshold, the computer automatically reduces the plotting sensitivity of 6 db and adjusts the amplitude within the threshold. If the amplitude still exceeds the maximum threshold, additional 6 db reduction is executed. The number of sensitivity reductions is shown by the number of horizontal lines shown adjacent to the seismogram. On St. 2, for instance, the portion covered by 2 lines illustrate the reduction of amplitude 2 x 6 db = 12 db (or 2^2 = 4 times). The plotting continues until the amplitude of the signal gradually diminishes. When the plotting is completed, the computer system prints out the epicenter, depth, origin time and magnitude as shown in Figures 3C-3F.

4. SEISMIC DATA RECORDED BY THE DAULE-PERIPA SEISMOGRAPH NETWORK

4.1 Data

The Daule-Peripa Seismograph Network was installed and started its first operation on 24 May 1982. This system operated until 24 October 1982 when the power supply for the printer/plotter failed. Due to prolonged procedures to clear the repaired equipment from Customs and subsequent malfunction of TTY, the network was not operating until 11 April 1983.

The data base now available are as follows:

(a) 24 May 1982 through 24 October 1982, and

(b) 11 April 1983 and thereafter.

As described in the section 3.1, station 4 did not get the data link until 11 April 1983, and RF transmission from station 6 was very weak and marginal until September 1982. Therefore the quality of data from 24 May 1982 through 24 October 1982 was less than originally designed.

The data from 11 April 1983 through 30 May 1983 was received by this office on 20 June 1983. We are working on this data, but due to tight time limits to deliver this report before the end of June, we have to confine our interpretation and discussion based only on the data from 24 May 1982 through 24 October 1982. A supplement of the report which includes interpretations of the latest data will be submitted within a month. Table 4 shows the list of earthquakes that occurred during the period of 24 May 1982 through 24 October 1982.

4.2 Shallow Depth Earthquakes

Figure 4A shows the shallow depth earthquakes (0-50 km) recorded by the Daule-Peripa network during the period from 24 May 1982 through 24 October 1982. The earthquakes between 78° - 81°W and 0°20' - 2°40'S are illustrated in this figure. The events in Figure 4A show widely scattered patterns, but one can recognize in this figure that the lineaments with northeast-southwest orientation started to emerge.

The most significant and important lineament shown in this figure is one passing through the immediate vicinity of the dam site and station 1 and extending southwest (in this text, this lineament is referred to as the Daule-Peripa Lineament). Another, and less significant trend may be recognized southeast of the former, which is passing through station 7 and running north of station 4.

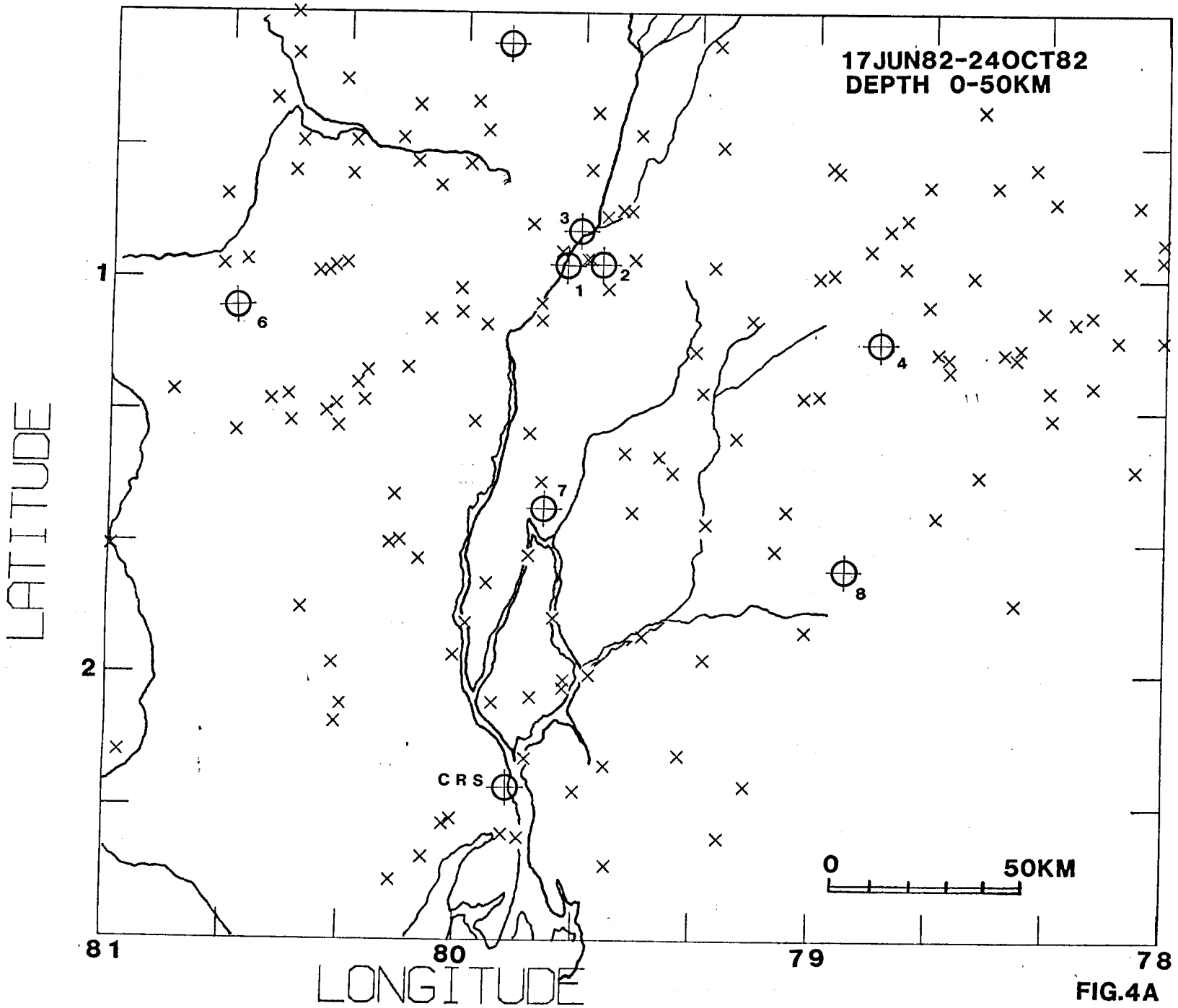

FIG.4A

RMS LT 1.5 DEP LT 50 ALL MAG*

Scant seismic information in this area makes it very difficult to establish a seismotectonic interpretation of the Daule-Peripa Lineament, but the following are some of the possible explanations for this northeast trend:

(a) The Benioff zone in this region is believed to be subducting toward the southwest. The orientation of the seismic trend is roughly perpendicular to the slip vector, and possible bending of the subduction plate affects stability of overlaying slab.

(b) South of Quito, the major geographical trends (including western Andes, Quito-Cuenca Depression, Cordillera Real, and eastern Andes) are approximately oriented north to south. Near Quito, however, this trend abruptly changes its orientation and runs northeast at the north of the equator. Orientation of this northeasterly trend is approximately parallel to the trend of the seismic lineaments. More importantly, if we extend the northern and southern margins of the depression between western Andes and eastern Andes towards southwest of Quito, we can observe that the two seismic lineaments described above are situated along the extension of northern and southern boundaries of the depression.

(c) Careful inspection of topograph maps (best shown by "mapa geografico, 1:500,000") reveals that there are significant alignment of topographic contours with northeasterly orientation at southwest Quito. One of the examples is shown by an arrow marked at the upper right-hand corner of Figure 4B. (Along the line of Rio Toachi Grande-Cordilleria de Lelin-Alluriquin: This lineament feature is situated along the extension of the southern margin of the depression.

STAND-ALONE PLOT IMAGES

FIG. 4B

STAND-ALONE PLOT IMAGES

Utsu (1968), among others, delivered the relation between the surface wave magnitude Ms and the length of the rupture zone l as follows:

$$Ms = 2 \log l(km) = 3.6$$

The Daule-Peripa Lineament, trending northeast and passing through the vicinity of the Dam site extends to approximately 110 km. At this writing, it is not clear how close this active trend runs from the project site. However, due to its length, it certainly constitutes the most serious potential hazard to the safety of the dam.

Assuming that the entire length of the active zone ruptures with a single event, and applying the observed length of l - 110 km, the largest earthquake which may occur along this zone is estimated at Ms = 7.68.

4.3 Intermediate Depth Earthquakes

Figure 4C shows earthquakes with a depth greater than 50 km. Similar to Figure 4A, one can observe two possible lineaments with northeast-southwest orientation. Location of these lineaments as compared to those shown in Figure 4A shifted approximately 30 km southeast implying that the Benioff zone is dipping southeast.

The projection of hypocenters onto the vertical plane trending east-west and north-south are demonstrated in Figures 4D and 4E respectively. Features we can observe from these figures are as follows:

(a) The event with the maximum depth is located at 180 km. Lack of events with depth greater than 200 km support the previously known quiescence of the seismicity along the Benioff zone in the depth range of 250 km to 550 km in this region.

(b) The configuration of the Benioff zone is not well defined in these figures. This is probably due to inadequate orientations on which we prepared the projections. Further study is needed to delineate the configuration of the Benioff zone.

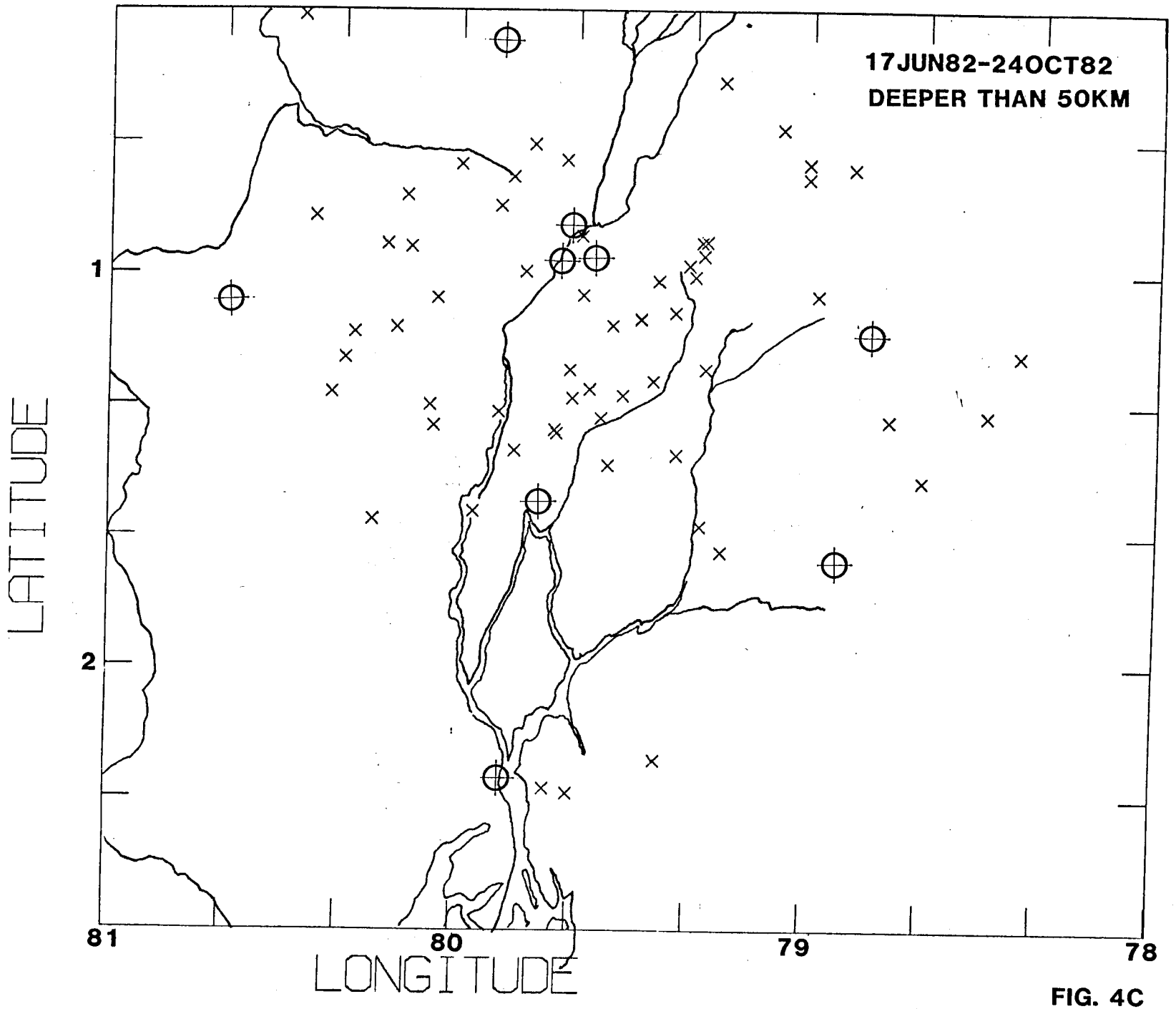

FIG. 4C

RMS LT 1.5 DEP GT 50 ALL MAG

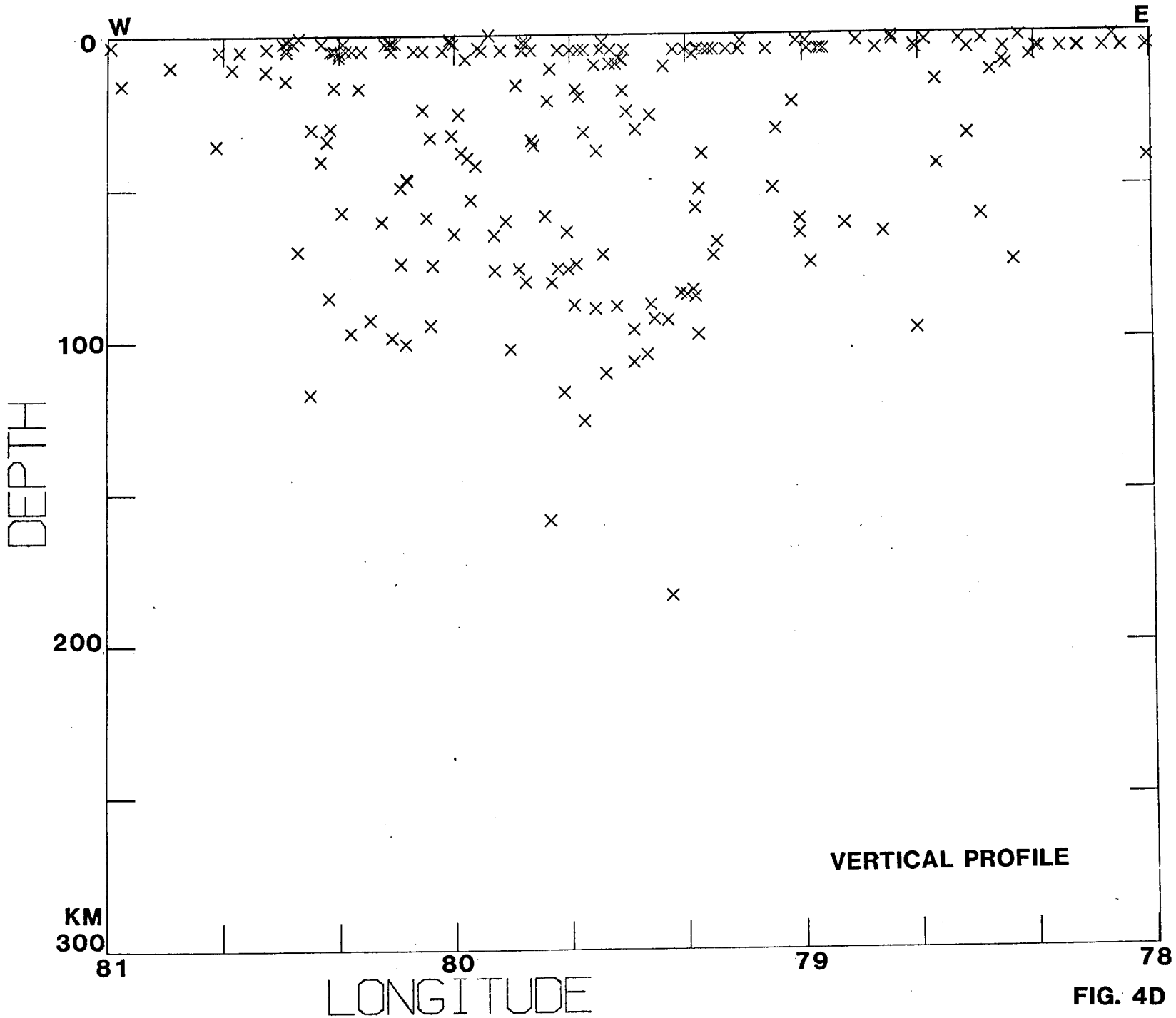

FIG. 4D

EW DEP PROFILE RMS LT 1.5 ALL MAG

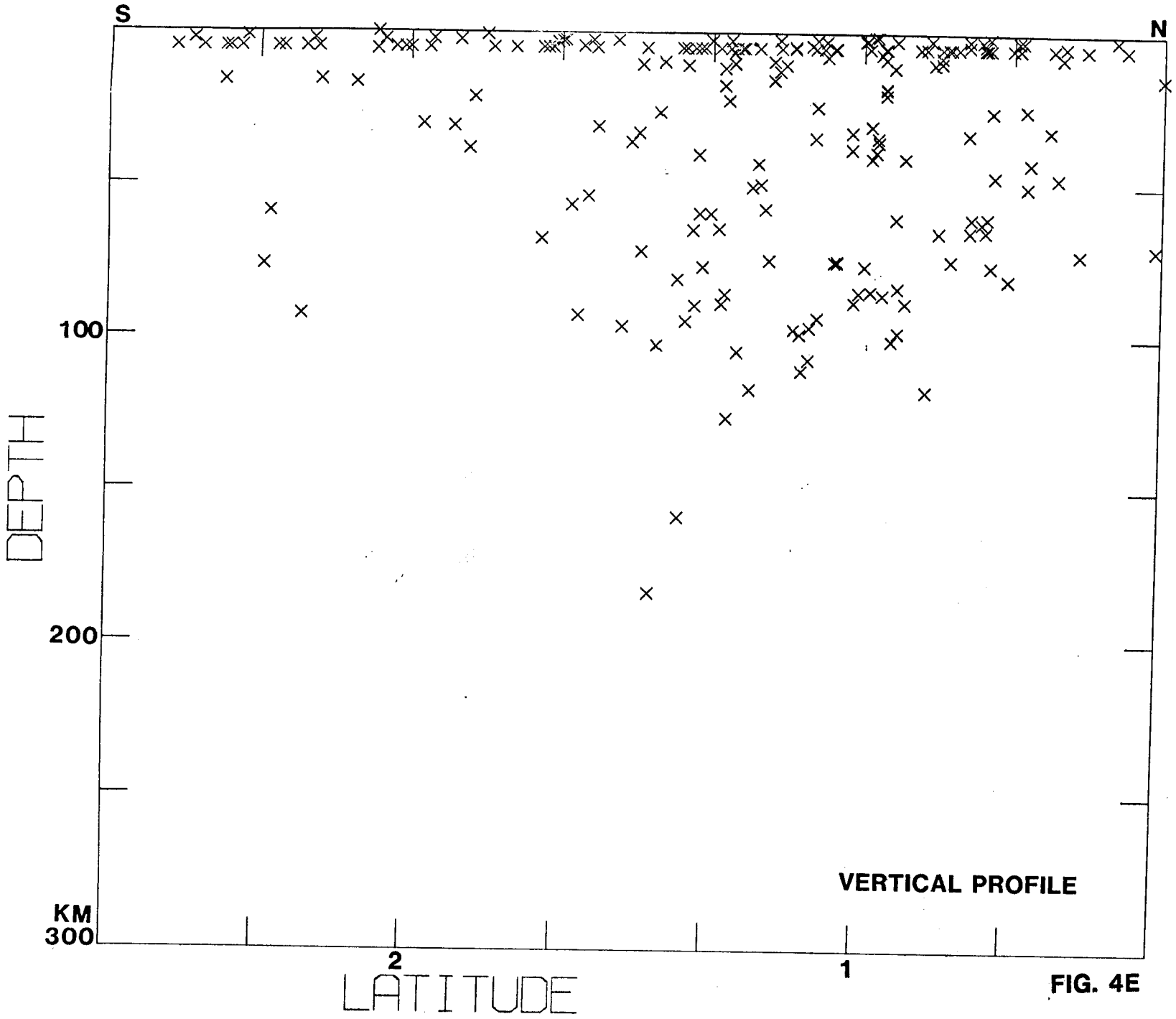

FIG. 4E

SN DEP PROFILE RMS LT 1.5 ALL MAG

5. CONCLUSION AND RECOMMENDATIONS

5.1 Conclusion

5.1.1. The Daule-Peripa Seismograph Network was established on 24 May 1982.

5.1.2. Problem of printer/plotter and TTY brought this operation to a stop on 24 October 1982. The network was repaired and brought back to operation on 11 April 1983.

5.1.3. During the period from 24 May 1982 through 24 October 1982, 287 events were recorded. Preliminary analysis indicated that there is an active seismic lineament (referred to as the Daule-Peripa Seismic Lineament) running near the dam site.

5.1.4. This active lineament runs northeast-southwest and extends over a length of up to 110 km long. If the total length of the active lineament ruptures with a single event, it may generate an earthquake up to surface wave magnitude Ms = 7.7.

5.2 Recommendations

5.2.1. Continued seismic monitoring is recommended. With continued monitoring, we hope to study

(a) refine the seismic lineament with the special emphasis of the Daule-Peripa Lineament

(b) establish the pattern of the seismic activity of pre-loading stage

(c) more detailed seismotectonic studies including fault plane solutions and configuration of the Benioff zone

5.2.2. More effective operation of the network can be achieved by:

(a) Improvement of importation procedure. Combined total of more

than 5 months of recording time was lost due to delay in importation procedure (Jan-Mar 1982 and Dec 82-Jan 83).

(b) Closer communication and more frequent shipment of the data.

REFERENCES

Baragangi, M. and B. L. Isacks (1976). Spatial distribution of earthquakes and subduction of the Nazca plate beneath South America Geology, 4, 686-692

Dewey, J. W. (1972). Seismicity and tectonics of western Venezuela, Bull. Seism. Soc. Am. 62, 1711-1751.

Fedotov, S. A. (1965). Regularitites of the distribution of strong earthquakes of Kamchatka, the Kurile Islands, and northeastern Japan, Tr. Inst. Fig. Zemli Akad. Nauk SSR, 36, 66-93.

Isacks, D. and P. Molnar (1971). Distribution of stresses in the descending lithosphere from a global survey of focal-mechanisms solutions of mantle earthquakes, Rev. Geophys. and Space Physics, 9, 102-174.

Kelleher, M. (1972). Rupture zones of large South American earthquakes and some predictions, J. Geophys. 77, 2087-2103.

Kelleher, M., L. Sykes and J. Oliver (1973). Possible criteria for predicting earthquake locations and their application to major plate boundaries of the Pacific and the Caribbean, J. Geophys. Res. 78, 2547-2585.

Kelleher, M., and w. McCann (1976). Boyant zones, great earthquakes and unstable boundaries of subduction, J. Geophys. Res., 81, 4885-4896.

Lomnitz, C. (1974). Global tectonics and earthquake risk, Amsterdam, New York, Elsevier Scientific Pub. Co. 320 pp.

Mogi, K. (1968). Sequential occurrences of recent great earthquake, J. Phys. Earth, 16, 30-36.

Pennington, W. (1981). The subduction of the eastern Panama Basin and the seismotectonics of northwestern South America, J. Geophys. Res., 86, 10753-10770.

Pennington, W. (1983). The effect of oceanic crustal structure on seismicity and subduction, in press, Tectonophysics.

Santo, T. (1969). A short study on the earthquake swarm in Galapagos Islands region in June 1968, Bull. Inter. Inst. Seis. Earthq. Engg., 6, 39-43.

Sato, Y. and D. Skoko (1965). Optimum distribution of seismic observation point, Bull. Earthq. Res. Inst., 43, 451-470.

Utsu (1968). Seismic activity in Hokkuido and its vicinity, Geophys. Bull., Hokkaido Univ., Japan, 20, 51-57.

Table 4 List of Earthquakes recorded by

The Daure-Peripa Seismograph Network

24 May 1982 - 24 Oct 1982

Y M D	H M	S	LAT	LON	D	RMS
820525	1124	40.57	-0.822	-79.552	5.00	0.40
820526	246	17.54	-1.702	-80.118	5.00	0.07
820526	440	16.64	-2.289	-79.668	5.00	0.09
820601	1912	35.21	-0.319	-79.004	5.00	1.39
820602	1113	39.80	-0.914	-79.299	97.98	0.30
820603	2329	37.49	-0.949	-80.620	5.00	0.41
820604	1529	23.46	-1.181	-78.649	2.25	0.56
820604	1649	45.40	-0.575	-78.528	5.00	0.34
820604	1731	0.03	-1.301	-80.545	11.48	0.66
820525	1154	16.80	-2.028	-79.703	5.00	0.34
820601	2059	13.22	-1.367	-80.351	5.00	1.28
820603	2015	43.46	-0.729	-78.880	62.06	0.61
820603	2253	40.65	-0.713	-78.958	5.00	1.13
820605	233	37.14	-0.961	-80.688	35.72	0.01
820608	113	0.18	-1.521	-78.673	96.46	0.48
820608	226	55.28	-0.721	-79.644	5.00	0.06
820608	1024	35.03	-1.661	-80.201	2.63	0.14
820608	1634	30.20	-0.899	-79.654	88.31	0.80
820608	1244	28.97	-0.965	-79.288	38.88	0.14
820609	625	55.48	-1.049	-79.648	74.92	0.55
820610	2314	14.84	-1.401	-79.719	80.91	0.32
820611	1 9	19.55	-1.368	-78.770	64.71	0.01
820611	17 4	46.41	-1.276	-78.331	5.00	0.03
820614	025	10.00	-0.802	-78.321	5.00	0.96
820614	043	59.41	-0.652	-80.467	2.50	0.66
820614	615	20.80	-0.928	-80.140	100.74	0.87
820614	1916	56.87	-2.051	-79.795	2.50	0.47
820615	1835	56.14	-0.344	-80.454	70.51	0.30
820619	1529	35.44	-1.126	-79.563	110.74	0.13
820619	1854	37.42	-0.977	-80.413	30.63	0.33
820619	2251	12.26	-0.808	-78.082	5.00	0.72
820620	0 6	45.95	-1.238	-79.296	50.55	0.61
820620	18 3	40.37	-0.701	-80.139	46.87	1.34
820620	1814	56.22	-1.475	-78.084	5.00	0.00
820620	2129	49.53	-0.963	-80.368	34.36	1.42
820621	534	11.14	-0.412	-79.284	5.00	1.48
820622	124	50.80	-1.346	-78.323	5.00	0.31
820622	2 4	13.71	-1.288	-80.497	2.50	0.27
820622	437	31.11	-0.751	-79.853	60.65	0.00
820622	1333	46.09	-0.643	-80.181	2.50	1.14
820623	1735	42.23	-1.259	-80.298	5.00	0.57
820624	1423	44.97	-0.044	-79.004	5.00	0.43
820624	1641	24.44	-0.732	-80.324	2.50	0.32
820625	714	50.29	-0.923	-78.845	2.50	0.30
820625	927	55.45	-0.632	-81.168	5.00	0.20
820626	0 9	6.14	-1.057	-79.781	5.00	0.08
820626	325	29.89	-0.188	-78.599	7.73	0.38
820626	439	48.70	-1.209	-80.325	57.67	0.22
820626	13 1	56.81	-1.263	-78.209	5.00	0.03
820626	2146	32.37	-0.946	-79.652	18.00	0.52
820626	2252	54.17	-2.224	-79.581	5.00	0.80
820629	1826	8.26	-1.046	-81.329	5.00	0.73
820630	521	44.19	-0.623	-79.940	42.50	0.33
820630	839	26.00	-2.513	-80.183	5.00	0.18
820630	852	30.06	-0.948	-79.519	8.29	0.26
820630	1324	31.47	-0.717	-79.009	60.41	1.20
820701	033	34.18	-1.226	-78.615	42.78	0.54
820703	1449	6.00	-0.824	-79.528	7.59	0.17
820706	2 1	24.32	-1.445	-79.840	102.57	1.04
820706	345	29.88	-1.851	-79.734	21.59	1.34
820706	923	15.91	-1.584	-79.512	5.00	0.51
820706	2010	43.94	-1.148	-78.008	4.58	0.03
820707	1237	52.27	-1.289	-79.627	126.40	0.29

820707	1444	28.95	-1.763	-79.924	5.00	0.78
820707	2228	11.20	-1.580	-79.076	30.99	0.46
820709	20	7 51.01	-0.562	-80.136	47.34	0.38
820709	2022	19.34	-0.798	-80.154	74.43	0.28
820710	114	38.92	-1.239	-79.684	116.83	0.28
820710	1326	9.32	-0.901	-78.011	41.03	0.23
820711	311	9.62	-0.946	-79.643	20.12	0.30
820711	856	58.33	-1.111	-79.933	4.05	1.46
820711	1047	45.92	-0.850	-80.415	117.32	0.23
820711	1320	0.51	-1.482	-79.571	71.68	0.83
820712	11	4 38.22	-1.863	-79.980	38.35	0.50
820712	2024	42.35	-1.692	-79.806	5.00	0.87
820713	039	52.19	-1.019	-79.592	38.06	0.49
820713	1441	17.58	-1.945	-80.014	2.25	0.60
820713	1636	18.38	-1.680	-79.106	5.00	0.83
820713	1916	0.12	-0.839	-79.598	10.02	0.10
820713	1918	33.94	-0.715	-78.378	1.25	0.52
820714	439	3.10	-1.346	-79.885	76.68	0.34
820714	1934	14.33	-0.927	-79.726	11.20	0.02
820716	956	54.60	-0.642	-81.140	5.00	0.70
820719	2338	44.34	-1.131	-80.180	98.77	1.31
820720	115	5.06	-0.972	-78.108	1.35	0.85
820721	2117	59.76	-0.823	-79.555	9.55	0.10
820721	2213	44.91	-1.490	-78.528	33.03	0.24
820721	2325	23.54	-0.965	-78.745	1.13	1.05
820722	2338	17.20	-1.305	-79.532	88.69	0.62
820723	1720	18.91	-1.019	-80.008	32.54	0.18
820723	1855	15.77	-1.200	-78.396	74.41	0.18
820724	1216	41.57	-1.099	-79.179	2.25	0.51
820728	6	9 58.40	-0.846	-78.744	2.25	0.44
820728	823	35.62	-2.358	-80.015	1.35	0.53
820729	1739	43.43	-0.956	-80.336	6.79	0.21
820730	1	0 45.27	-2.455	-80.094	5.00	0.24
820730	1	6 55.48	-1.814	-78.422	5.00	0.16
820730	2347	57.94	-0.501	-80.344	5.00	0.27
820802	632	47.13	-1.293	-79.030	22.14	0.44
820802	15	3 52.24	-0.043	-78.187	96.96	0.25
820802	1436	14.97	-0.500	-81.112	6.10	0.18
820802	2040	23.05	-0.669	-79.794	80.70	0.23
820804	19	1 46.83	-1.539	-80.188	2.50	0.83
821006	1421	10.77	-1.484	-79.398	10.41	0.07
821006	1521	32.47	-2.405	-79.824	16.25	0.31
821007	234	46.70	-1.885	-79.020	2.52	0.82
821007	10	3 34.89	-0.975	-80.386	41.07	0.55
821007	1036	33.42	-1.965	-80.359	30.25	0.50
821007	1123	31.86	-0.707	-79.989	25.83	0.24
821008	1659	51.37	-1.312	-80.358	5.00	0.77
821011	1319	11.88	-0.871	-78.791	5.00	0.16
821012	1146	32.08	-0.630	-79.086	50.30	0.38
821013	1433	51.64	-1.382	-80.641	10.69	0.19
821013	1941	58.54	-1.655	-80.172	2.50	0.21
821013	1944	43.67	-2.231	-79.424	92.76	0.17
821014	1	8 12.30	-0.988	-78.550	2.25	0.45
820810	452	47.31	-1.614	-79.303	4.50	0.20
820810	827	54.74	-0.580	-79.628	31.96	0.14
820810	1249	9.34	-0.754	-79.009	65.04	0.35
820812	1738	53.08	-1.193	-78.426	9.27	0.18
820813	452	47.56	-1.061	-78.676	5.00	0.09
820813	456	13.28	-1.354	-78.488	59.37	0.09
820813	720	52.99	-0.946	-79.517	18.44	0.71
820813	8	7 5.05	-0.992	-78.991	2.50	0.09
820813	10	5 47.90	-1.330	-80.386	2.50	0.25
820815	027	56.57	-1.109	-79.484	96.51	0.17

820815	1018	18.96	-1.456	-79.378	183.85	0.92
820816	147	56.64	-1.672	-80.993	3.15	0.51
820816	236	21.33	-1.896	-79.480	31.10	0.91
820816	1516	19.62	-1.382	-80.070	94.53	0.58
820816	1232	13.81	-1.194	-78.619	15.49	0.62
820816	2121	58.64	-1.168	-78.415	10.31	0.48
820817	536	22.05	-1.434	-79.537	9.55	0.75
820817	1817	38.79	-2.007	-79.702	5.00	1.14
820817	2124	13.65	-1.356	-79.964	40.09	0.43
820818	317	22.71	-1.056	-80.063	74.97	0.52
820818	530	28.37	-0.726	-78.941	5.00	0.46
820819	1625	30.52	-1.145	-80.299	97.16	1.36
820822	15	1 13.23	-1.226	-80.271	5.00	0.74
820822	19	0 30.80	-0.983	-78.951	5.00	0.56
820822	21	4 0.55	-1.219	-80.157	49.67	0.61
820823	527	10.32	-0.708	-79.701	76.24	0.55
820823	9	5 21.70	-2.303	-79.740	59.13	0.35
820824	1134	3.85	-1.329	-80.081	59.42	0.62
820825	453	47.79	-0.220	-80.827	5.00	0.07
820825	839	10.69	-1.181	-78.461	12.56	0.66
820826	421	48.87	-2.115	-80.349	16.79	0.57
820826	523	9.73	-0.664	-79.270	5.00	0.12
820826	13	7 38.65	-0.760	-80.072	33.32	0.26
820829	6	6 34.08	-0.915	-79.312	83.38	0.93
820830	1550	48.27	-1.393	-79.726	158.97	0.37
820901	1623	31.25	-1.355	-80.486	5.00	0.61
820901	2042	50.63	-1.444	-79.438	26.17	0.52
820901	2313	2.50	-2.476	-79.576	2.50	0.34
820902	021	12.91	-0.719	-80.001	64.70	0.37
820903	2019	32.72	-1.701	-79.245	67.76	0.43
820904	1827	39.29	-1.050	-78.977	74.66	0.51
820904	23	7 21.92	-1.954	-79.304	5.00	0.02
820904	2322	16.28	-0.825	-79.886	65.12	0.43
820905	240	40.45	-0.331	-80.489	14.52	0.32
820905	410	22.79	-2.369	-80.037	5.00	0.51
820905	936	32.91	-1.827	-80.451	0.75	0.68
820907	1650	4.71	-0.725	-80.487	3.94	0.01
820907	1721	15.03	-1.594	-78.649	2.50	0.08
820907	1743	53.74	-2.405	-79.257	5.00	0.70
820908	252	35.07	-0.920	-80.209	60.76	0.84
820908	754	29.11	-0.761	-78.486	2.25	1.04
820909	112	38.21	-1.506	-79.772	36.01	0.91
820909	145	24.37	-1.385	-79.807	5.00	1.12
820909	3	5 54.04	-0.974	-79.347	84.47	0.27
820910	953	39.25	-1.297	-80.362	85.54	0.51
820911	327	43.13	-2.206	-79.806	2.50	1.13
820911	655	22.00	-1.282	-79.317	6.58	0.40
820911	8	3 27.35	-1.100	-79.778	34.33	0.20
820911	942	42.03	-0.945	-78.014	5.00	0.17
820911	1313	39.60	-1.599	-79.953	53.71	0.16
820911	1335	35.09	-1.302	-80.278	17.30	0.53
820911	1439	42.21	-0.761	-78.681	4.05	0.21
820911	2015	14.86	-2.065	-79.902	0.02	0.40
820912	18	5 41.73	-2.315	-79.672	76.51	0.61
820912	20	3 39.62	-0.554	-79.969	7.66	0.51
820912	2131	38.40	-1.147	-78.138	5.00	0.18
820913	1649	31.42	-1.110	-79.483	107.11	0.27
820913	1828	6.15	-1.178	-79.338	5.00	0.47
820913	20	6 9.40	-1.996	-79.628	5.00	0.30
820915	2026	32.33	-1.079	-80.005	2.64	0.55
820921	3	4 15.93	-0.227	-79.403	2.25	0.35
820921	1323	15.41	-0.230	-79.439	2.50	0.88
820922	536	5.32	-0.259	-79.406	5.00	0.80

820922	753	52.96	-1.289	-78.987	5.00	0.92
820922	2034	50.04	-1.363	-79.594	89.45	0.45
820923	1212	28.24	-1.395	-79.220	5.00	0.35
820924	1620	29.78	-1.268	-79.445	104.68	0.73
820927	2040	2.50	-2.396	-79.868	5.00	1.26
820927	2041	38.68	-1.102	-78.259	5.00	0.40
820928	1157	22.43	-3.122	-79.797	5.00	0.05
820929	2212	21.70	-0.436	-80.484	1.75	0.26
820930	1250	1.72	-1.084	-78.213	5.00	0.33
820930	1340	0.27	-0.067	-78.778	5.00	0.46
820930	2112	10.43	-1.311	-79.677	64.35	1.00
821001	2246	17.77	-2.193	-80.960	15.81	0.86
821005	437	38.92	-0.949	-79.307	85.57	0.33
821005	1940	20.52	-0.989	-79.814	76.39	1.43
821005	2332	21.37	-1.093	-79.385	93.32	0.51
821015	1 7	35.53	-0.857	-79.808	5.00	0.06
821015	232	54.01	-0.512	-79.255	72.27	0.02
821015	426	37.02	-1.076	-78.349	7.68	0.96
821015	7 3	46.14	-0.785	-80.681	5.00	0.68
821015	1023	24.27	-1.280	-80.821	9.93	0.86
821015	1211	5.42	-1.097	-80.094	24.20	0.04
821015	1911	44.31	-0.548	-80.543	4.05	1.24
821018	1213	31.07	-2.275	-79.184	5.00	0.42
821018	1119	39.09	-1.620	-80.243	92.86	1.42
821019	15 3	46.07	-2.069	-80.334	5.64	0.07
821019	1830	59.97	-1.001	-79.330	84.95	0.30
821020	450	44.21	-2.197	-79.372	5.00	1.19
821021	1953	1.96	-1.636	-79.306	56.56	0.05
821022	2250	4.64	-0.634	-79.505	25.16	0.90
821022	2256	36.89	-1.012	-79.434	88.11	0.17